[redacted]

[redacted] 390 2

Copy

RM E51K23

NACA RM E51K23

RESEARCH MEMORANDUM

COOLING CHARACTERISTICS OF AN EXPERIMENTAL TAIL-PIPE BURNER WITH AN ANNULAR COOLING-AIR PASSAGE

By William K. Koffel and Harold R. Kaufman

Lewis Flight Propulsion Laboratory
Cleveland, Ohio

[redacted]

NATIONAL ADVISORY COMMITTEE
FOR AERONAUTICS

WASHINGTON
February 26, 1952

[redacted]

 [redacted]

2408

NATIONAL ADVISORY COMMITTEE FOR AERONAUTICS

RESEARCH MEMORANDUM

COOLING CHARACTERISTICS OF AN EXPERIMENTAL TAIL-PIPE

BURNER WITH AN ANNULAR COOLING-AIR PASSAGE

By William K. Koffel and Harold R. Kaufman

SUMMARY

The effects of tail-pipe fuel-air ratio (exhaust-gas temperatures from approximately 3060° to 3825° R), radial distribution of tail-pipe fuel flow, and mass flow of combustion gas on the temperature profiles of the combustion gas and on temperature profiles of the inside wall of the combustion chamber were determined for an experimental tail-pipe burner cooled by air flowing through an insulated cooling-air passage 1/2 inch in height. The effects on inside-wall temperature of varying the mass-flow ratio of cooling-air to combustion-gas mass flow from approximately 0.067 to 0.19, inlet cooling-air temperature from about 520° to 1587° R, and combustion-gas mass flow from 22.3 to 13.8 pounds per second were also determined.

Large circumferential variations existed in the combustion-gas temperature near the inside wall. These variations resulted in similar variations in the inside-wall temperature. The circumferential variations formed consistent patterns that were similar, although different in magnitude, for all configurations tested.

The two extremes in radial distribution of tail-pipe fuel flow, high fuel concentration toward the combustion-chamber wall and high fuel concentration in the center of the combustion chamber, changed the circumferential average inside-wall temperature 235° F at a station 48 inches downstream of the flame holder. The configuration having a high fuel concentration near the wall presented a more severe cooling problem as the circumferential variation was greatest for this configuration.

The spread of flame to the inside wall, as determined from measurements of combustion-gas temperature near the wall, was practically unaffected by fuel-air ratio. However, the flame spread to the wall was a function of radial fuel distribution. At no time did the flame impinge on the wall within 24 inches downstream of the flame holder. Radiant heat transfer to this section of the inside wall was insufficient to require wall cooling in the first 24 inches, if the tail-pipe materials could withstand nonafterburning operation without cooling.

[redacted]

With the most uniform distribution of tail-pipe fuel tested and an inlet cooling-air temperature of 520° R, an average inside-wall temperature of 1300° F at a station 48 inches downstream of the flame holder required mass-flow ratios of 0.12 and 0.09 with exhaust-gas temperatures of 3825° and 3435° R, respectively. When the distance was increased to 56 inches downstream of the flame holder, a mass-flow ratio of 0.115 was necessary with an exhaust-gas temperature of 3435° R.

At a mass-flow ratio of 0.145, the inside-wall temperature 48 inches downstream of the flame holder was increased about 4/10° per degree increase in inlet cooling-air temperature.

The temperature of the structural wall of an insulated tail-pipe burner having an inner liner would be practically the same with or without tail-pipe burning.

INTRODUCTION

The combustion-chamber walls of tail-pipe burners must either withstand high operating temperatures or be cooled to temperatures that give adequate strength and service life. The trend toward nonstrategic materials and improvements in performance and the operating range of tail-pipe burners have made cooling more critical. Many methods have been considered for cooling the walls of a tail-pipe combustion chamber including the flow of air through an annular passage surrounding the combustion chamber, the flow of turbine outlet gas through an annular passage formed by a concentric inner liner, the establishment of a cool-air film between the walls and the combustion gas by means of a porous wall or a series of annular nozzles, as well as ceramic coatings and fuel additives that coat the walls and reduce the radiant heat transfer to the walls or lower the wall temperature by their insulative properties. Many combinations of these methods have been and are being investigated at the NACA Lewis laboratory. Considerable attention has been given to the annular cooling-air shroud and to the inner liner and to their use in combination.

An analytical method was developed (reference 1) for calculating the maximum average wall temperature in tail-pipe combustion chambers cooled by the parallel flow of air through an annular cooling passage or cooled by turbine discharge gases flowing between an inner liner and the combustion-chamber wall. The method was based on the simplifying assumptions of a uniform transverse temperature profile, a linear rise in combustion-gas temperature from flame holder to exhaust-nozzle exit, and the fact that radiation from the combustion gas to the wall was twice the nonluminous radiation of a completely burned stoichiometric mixture of octane and air. Wall temperatures or cooling-air flows calculated by the method of reference 1 have checked well with values

[redacted]

measured on experimental tail-pipe burners in which a uniform transverse temperature profile was approached. Agreement was poorer for burners producing nonuniform profiles. Some effects of changing the flame-holder design and tail-pipe fuel distribution, and consequently the transverse temperature profile, are given in reference 2.

The cooling and pumping characteristics of a tail-pipe burner having an inner liner and an external cooling-air shroud with an ejector nozzle are presented in reference 3, and an analytical method is developed in reference 4 for predicting the pressure drop through the cooling passages. These investigations on tail-pipe-burner cooling had limited ranges of cooling-air flows and inlet cooling-air temperature and no attempt was made to determine the combustion-gas temperature profiles as effected by changes in internal configuration and to relate them to the temperatures of the combustion-chamber walls.

This report includes some results of an experimental investigation on a tail-pipe burner which was extensively instrumented. Ranges of independent control of the cooling-air temperature, flow, and pressure, as well as the combustion-gas temperature and flow wider than those given in the references are presented herein. The data presented were obtained with a combustion chamber having a constant-flow area and an annular cooling passage of constant height. The effects of exhaust-gas temperature level, distribution of tail-pipe fuel across the turbine annulus, and mass flow of combustion gas on the temperature profiles of both the combustion gas and the inside wall are presented.

APPARATUS

Engine

A conventional and axial-flow turbojet engine was used in this investigation. The sea-level static thrust of the engine was approximately 3100 pounds at a rated engine speed of 12,500 rpm and a maximum turbine-outlet temperature of approximately 1200° F (1660° R). At this condition the air flow was slightly less than 60 pounds per second.

The fuel used in the engine and the tail-pipe burner was MIL-F-5572, grade 80, unleaded gasoline and had a lower heating value of 19,000 Btu per pound and a hydrogen-carbon ratio of 0.185.

Installation

The standard tail pipe was replaced by an experimental tail-pipe-burner assembly attached to the turbine flange. The engine and the tail-pipe burner were mounted on a wing section in the 20-foot-diameter

[redacted]

test section of the altitude wind tunnel. Refrigerated air was supplied to the compressor inlet through a duct from the tunnel make-up air system. This duct was connected to the engine with a labyrinth seal, which made possible measurement of thrust with the tunnel balance system. Air was throttled from approximately sea-level pressure to the desired pressure at the compressor inlet; while pressure in the tunnel test section was maintained at the desired altitude. Cowlings and fairings were omitted from the engine and the tail-pipe burner in order to simplify the installation and to facilitate inspection and servicing of engine, 2408
tail-pipe burner, and instrumentation.

Tail-Pipe-Burner Assembly

The entire tail-pipe-burner assembly was fabricated of 1/16-inch Inconel. The over-all length of the engine and tail-pipe burner was approximately 16.1 feet, of which the tail-pipe diffuser, the combustion chamber, and the nozzle were 2, 5, and 1 feet, respectively. Figure 1 is a schematic drawing of the installation showing the fuel-spray bars in the annular diffuser, the cylindrical combustion chamber with insulated cooling passage, and the fixed-conical exhaust nozzle. The flame holder had a single V-gutter with sinusoidal corrugations on the trailing edges. The V-gutter had a mean diameter of 18 inches, a mean width across the corrugations of $1\frac{3}{4}$ inches, and an included angle of 35°. The blockage at the downstream face of the flame holder was about 23 percent and the velocity at the flame holder under the conditions of this investigation was approximately 480 feet per second. The cooling passage had a constant height of 1/2 inch and was insulated with 1 inch of refractory cement.

Fuel-spray bars. - Twelve radial fuel-spray bars were equally spaced 8.75 inches downstream of the turbine flange and 13.25 inches upstream of the flame-holder center line. Each bar had seven holes (number 76 drill) that sprayed fuel normal to the gas flow. Three different sets (twelve bars per set) of spray bars were used to vary the fuel distribution across the turbine discharge annulus. The first set (fig. 2(a)) produced a nearly uniform fuel distribution with a slightly higher fuel concentration at the very center for flame stability and piloting action. The second set (fig. 2(b)) increased the fuel concentration toward the combustion-chamber wall and decreased the fuel flow in the center of the combustion chamber. The third set of spray bars (fig. 2(c)) concentrated more fuel at the center and decreased the fuel concentration near the combustion-chamber walls.

Configurations. - The three sets of fuel-spray bars were used in combination with four different exhaust nozzles to form essentially three configurations as follows:

Configuration	Fuel-spray bars	Exhaust-nozzle exit area (sq ft)	Figure
A	Set 1	1.846 1.903 1.980 2.160	3(a)
B	Set 2	1.903	3(b)
C	Set 3	1.903 2.160	3(c)

INSTRUMENTATION

Because it was recognized that the combustion pattern would be irregular and the temperatures to be measured were severe on thermocouples, as many thermocouples as practicable were used in order to obtain representative average temperatures and to provide sufficient thermocouples if some thermocouples should fail. Six instrumentation stations, B to G (fig. 3), were provided along the length of the cylindrical combustion chamber. Thermocouples were installed at station B for measurement of the inlet cooling-air temperature. Stations C to F had six groups of instrumentation, equally spaced around the circumference, for measuring the temperatures of the inside and outside walls of the tail-pipe burner and of the cooling air as well as the static and total pressures of the cooling air. The temperatures of the inside and outside walls were also measured at four points around the circumference at station G, and the cooling-air temperatures and pressures at station G were measured in the discharge ducts on the downstream plenum chamber. The locations of the instrumentation at each of these stations, at the exhaust nozzle, the cooling-air metering nozzle, and the upstream plenum chamber are shown in figure 4. The cross section of a typical group of instrumentation at stations C through F is shown in figure 5.

The means of providing for longitudinal movement due to thermal expansion can be seen in figure 5. The platinum-rhodium - platinum thermocouple probes extended through sliding seals in the outside wall and the sliding channels connecting the inside and outside walls permitted longitudinal movement of the walls.

The usual pressure and temperature instrumentation was installed at several measuring stations through the engine. Fuel flows to the engine and tail-pipe burner were measured with calibrated rotameters.

Wall-temperature measurement. - The temperature of the inside wall of the tail-pipe burner was measured with chromel-alumel thermocouples spot-welded to the outer surface of the wall (fig. 5). Conductive cooling of the junction was reduced by strapping the leads to the wall for 3/4 inch downstream of the junction before extending the leads across the cooling passage. The temperature of the outside wall was measured by a chromel-alumel thermocouple welded into the head of a hollow oval-headed screw (fig. 5). Conductive cooling of the junction was negligible because the stem of the screw was buried under the cooling-passage insulation.

<u>Cooling-air temperature measurement</u>. - The cooling-air temperatures were measured by means of National Bureau of Standards type (fig. 6) shielded thermocouples (reference 5). The radiation shield consisted of a 1/4-inch length of 1/8-inch silver tubing which was slid over the bare junction and compressed to a biconvex airfoil section.

<u>Combustion-gas temperature measurement</u>. - Combustion-gas temperatures near the inside wall were measured by means of the platinum-rhodium - platinum thermocouples shown in figure 7. Each thermocouple probe had a water-cooled supporting stem and two thermocouples in parallel having a common hot junction. The leads from the junction were arranged in a cross to give mechanical support at high temperatures. Negligible conduction error was obtained by means of the high length-diameter ratio of the leads between the junction and the cooled supporting stem. No radiation shield was used because of the low emissivity and absorptivity of the platinum and platinum-rhodium wires.

Gas temperature profiles at station F were obtained by means of a rake having seven sonic-flow orifice temperature probes (fig. 8). The temperature of a gas sample flowing into one of these probes is obtained from a thermodynamic equation and is theoretically independent of radiation effects (see reference 6).

The exhaust-gas temperature was computed (as given in appendix A) from rake measurements of total pressure at the exhaust-nozzle exit and the measured gas flow.

Accuracy

Four flight recorders were used because of the large number of thermocouples and in order to reduce the recording time while maintaining equilibrium conditions. The estimated over-all accuracy of the temperature measurements are as follows:

Wall temperature, °F	±15
Cooling air, °F	±10
Gas temperatures near the wall, °F	±20
Sonic-flow orifice probe, °F	±150
Exhaust gas temperature, °F	±50

PROCEDURE

The geometry of the tail-pipe diffuser and the flame holder in combination with the fuel-spray bars producing approximately uniform distribution of fuel across the turbine annulus (configuration A) was shown, in preliminary tests on a similar burner, to give good performance and operating characteristics over a wide range of altitudes and fuel-air ratios. Cooling characteristics of the experimental tail-pipe burner were obtained with the seven combinations of exhaust-nozzle exit area and fuel-spray bars, at pressure altitudes of 30,000 and 40,000 feet, a flight Mach number of 0.52, and an engine speed of 12,500 rpm. It was impossible to run the tests at lower pressure altitudes because the flow of dry cooling air, at approximately atmospheric pressure from outside the tunnel, was dependent on the difference in the atmospheric pressure and the pressure in the tunnel test section. Dry refrigerated air was supplied to the engine at $505^\circ \pm 5^\circ$ R. The total pressure at the engine inlet was regulated to correspond to the desired pressure at each altitude with complete free-stream total-pressure recovery.

Most of the data were obtained by adjusting the tail-pipe fuel flow to maintain an average turbine-outlet temperature of $1633^\circ \pm 12^\circ$ R; an approximately constant exhaust-gas temperature was thus obtained for each nozzle-exit area and mass flow. The remainder of the data were taken at lower turbine-outlet temperatures.

The cooling-air flow and the cooling-air temperature were systematically varied while holding all other quantities constant.

The approximate range of variables investigated with a limiting turbine-outlet temperature of 1633° are given in the following table:

Configuration	Altitude (ft)	Exhaust-gas temperature T_g (°R)	Combustion-gas flow W_g (lb/sec)	Mass ratio W_a/W_g	Cooling-air inlet temperature T_a (°R)
A	30,000	3060	22.1	0.0672 to .1872	500 to 1587
	30,000	3240	22.2	0.1002 to .1917	500 to 1222
	30,000	3435	22.3	0.0953 to .1796	502 to 1408
	40,000	3265	13.8	0.1440	528 to 1340
	30,000	3825	22.8	0.1374 to .1906	515
B	30,000	3215	22.2	0.0985 to .1891	495 to 1223
C	30,000	3235	22.3	0.1420	524 to 1450
	30,000	3764	22.4	0.1912	524

The cooling-air mass flow was controlled by flap valves on the outlet ducts of the downstream plenum chamber. The static pressure in the cooling passage was balanced against the static pressure of the combustion gas at station F by means of pressure-regulating valves upstream of the air-metering nozzle in conjunction with the flap valves. When the pressures were balanced, large pressure forces were transferred from the hot, and consequently weaker, inside wall to the cooler outside wall. This transfer tended to minimize any changes in cooling-passage height. The cooling-air temperature was varied by means of a turbojet can-type combustor in the cooling-air supply duct downstream of the air-metering nozzle.

RESULTS AND DISCUSSION

Typical results of this cooling investigation are presented graphically and the performance of the three configurations are tabulated in tables I and II. The effects of exhaust-gas temperature level, radial distribution of tail-pipe fuel flow, and combustion-gas mass flow on the temperature profiles of the combustion gas are presented first because of the influence these profiles have on the temperatures of the inside wall.

Reproducibility of Combustion-Gas Temperature Profiles

Circumferential profiles. - The combustion-gas temperatures near the inside wall, the temperature of the inside and outside walls of the cooling passage and the cooling-air temperature are plotted against the group positions around the circumference at station F in figure 9. The reproducibility of the data is indicated in figures 9(a) to 9(c) for a check point having an exhaust-gas temperature of approximately 3060° R, mass-flow ratio of 0.098, and an inlet cooling-air temperature of 530° R. The profiles are similar as the accumulated afterburner time increased from 32 minutes to 9 hours and 22 minutes. The profiles with an exhaust-gas temperature of 3484° R (fig. 9(d)) are similar although the temperature levels are higher. The profiles shown in figure 9 were obtained with the first set of fuel bars, which produced the most uniform fuel distribution. The reproducibility shown is typical of data obtained with the other configurations. The large variations in gas temperatures around the circumference are reflected in the inside-wall temperature. The difference between the highest and the lowest gas temperatures around the circumference, as measured by the platinum thermocouples at station F, was approximately 500° to 900° F, and the difference for the inside-wall temperatures was about 400° to 600° F. The larger circumferential variations in gas temperature are believed to be caused by assymetrical distributions in the engine fuel-air ratio and in turbine-discharge gas flows because daily inspections disclosed no plugging of the fuel-spray bars in the tail-pipe burner.

Longitudinal profiles. - Typical longitudinal profiles of the combustion-gas temperature measured by the platinum-rhodium - platinum thermocouples 1/2 inch from the inside wall are shown in figure 10. The general reproducibility of the combustion pattern for a given set of fuel-spray bars can be seen by comparing the relative positions of the temperature profiles for each circumferential group as the exhaust-gas temperature is increased (fig. 10). Similar reproducibility of the relative positions of each group was observed in the longitudinal profiles for the combustion-gas temperature measured 1/4 inch from the inside wall and for the temperature of the inside wall.

Inasmuch as the longitudinal temperature profiles for various circumferential positions reproduced in a consistent manner in spite of large circumferential temperature variations, the effects of exhaust-gas temperature, of fuel distributions, and of combustion-gas mass flow are based on circumferential average temperatures. (The temperatures in table II are circumferential averages.)

Effect of Variables on Average Longitudinal Profiles of Combustion-Gas Temperature

2408

Exhaust-gas temperature. - The effect of increased exhaust-gas temperature (or tail-pipe fuel-air ratio) and the spread of the flame toward the inside wall are shown in figure 11. The combustion-gas temperature within 1/4 inch of the wall (fig. 11(a)) remains at approximately turbine-discharge temperature as far downstream as station D indicating that, for the same fuel distribution, the spread of the flame toward the inside wall is practically unaffected by fuel-air ratio (exhaust-gas temperature level) although the transverse temperature gradients between stations C and D increase with fuel-air ratio as can be seen from figure 11(b). Consequently, no cooling would be required for configuration A in the first 24 inches downstream of the flame holder if the burner walls could withstand the nonafterburning operation without cooling. Downstream of this point, the cooling requirements increase as the transverse gas temperature gradients near the wall increase with both distance from the flame holder and with exhaust-gas temperature level.

Fuel distribution. - The effects of marked changes in tail-pipe fuel distribution across the turbine-discharge annulus on the gas temperatures near the inside wall are shown in figure 12. Figure 12(a) shows that the flame spreads out to the wall between 24 and 36 inches downstream of the flame holder depending on the radial distribution of fuel. The flame intercepted the wall first with configuration B, which had a high fuel-air ratio near the wall, and last with configuration C, which had a high fuel-air ratio in the center of the burner. The cooling problem apparently can be altered by changes in fuel distribution at a given exhaust-gas temperature level. It is not, however, always possible to alleviate the cooling problem by altering the radial distribution of fuel because of possible adverse effects on performance and operational characteristics of the tail-pipe burner. For example, configuration C produced low inside-wall temperatures with the third set of fuel-spray bars, and had very smooth combustion and the exhuast nozzle was colder than for configuration A at the same exhaust-gas temperature, but it was impossible to obtain a turbine-outlet gas temperature of 1633° R with these fuel-spray bars when the exhaust-nozzle exit area was 2.160 square feet. On the other hand, configuration B, which produced high inside-wall temperatures, was difficult to ignite, burned roughly, and blew-out whenever the turbine-outlet gas temperature dropped below 1615° R.

The corresponding changes in transverse temperature profiles with changes in fuel distribution will be discussed in the section Fuel Distribution.

Combustion-gas mass flow. - The effect of decreasing the combustion-gas mass flow on the gas temperatures near the inside wall is shown in figure 13. The decrease in mass flow of combustion gas from 22.29 to 13.85 pounds per second, resulting from increasing the altitude from 30,000 to 40,000 feet, lowered the combustion-gas temperatures between stations E and F, about 400° and 200° F at distances from the inside wall of 1/4 and 1/2 inch, respectively. These temperature reductions, however, would be about one-half as great if cross-plotted data from figure 11 were used to estimate the longitudinal temperature profile at the same exhaust-gas temperature as with the lower mass flow. The decrease in exhaust-gas temperature occurred because the tail-pipe fuel flow was adjusted for a constant indicated turbine-outlet gas temperature, but the mean turbine-outlet gas temperature decreased because of a change in the radial temperature profile as altitude was changed.

Variation of Gas Temperatures Near the Wall with Cooling-Air Flow and Temperature

The temperature of the combustion gas near the wall was affected slightly by the inside-wall temperature, and consequently, by the mass flow and the temperature of the cooling air. The influence of cooling-air flow and the inlet cooling-air temperature on the gas temperature measured 1/4 inch from the inside wall was found to be negligible at stations C and D. The effect of cooling-air flow at stations E and F is given by the approximate equation

$$\Delta T_{g,1/4} = 1000\,\Delta\left(\frac{W_a}{W_g}\right) \tag{1}$$

and the effect of inlet cooling-air temperature is about 1/10° per degree rise in inlet cooling-air temperature. (The symbols used are defined in appendix B.)

Effects of Variables on Transverse Gas-Temperature Profile at Station F

Some of the more representative transverse profiles of the combustion-gas temperature at station F were selected for presentation. The temperatures in the combustion zone were obtained by means of the sonic-flow orifice rake and the temperatures near the wall were measured by the platinum-rhodium - platinum thermocouples 1/4 inch from the inside wall.

Exhaust-gas temperature. - Transverse temperature profiles are shown for configuration A in figure 14. Temperature peaks in figure 14(a) corresponding to the wake of the single-V flame holder tend to disappear and the profile to become more uniform as the exhaust-gas temperature is increased (figs. 14(b) and (c)).

The gas temperatures 1/4 inch from the inside wall and in the center of the combustion zone increased 600° to 700° R as the average exhaust-gas temperature increased approximately 440° R.

Fuel distribution. - The effects of changing the radial distribution of fuel across the turbine annulus on the transverse profile of combustion-gas temperature are shown in figure 15. Figure 15(a) shows that the transverse temperature profile of configuration A at an exhaust-gas temperature of 3266° R had a temperature peak in the wake of the flame-holder gutter similar to the peaks existing at an exhaust-gas temperature of approximately 2926° R (fig. 14(a)). The high fuel concentrations near the inside wall in configuration B (fig. 15(b)) resulted in much higher gas temperatures near the inside wall at the bottom of the burner and the gas temperature at the center of the burner was greatly reduced because the tail-pipe fuel-air ratio and exhaust-gas temperatures were practically constant. The average gas temperatures 1/4 inch from the inside wall were approximately 400° R higher for configuration B than for configuration A at a mass-flow ratio of 0.143 and an exhaust-gas temperature of approximately 3240° R. The fuel distribution of configuration C moved the peak temperatures toward the center of the burner and the average gas temperature 1/4 inch from the inside wall was about 350° R lower than for configuration A at a mass-flow ratio of 0.143. For the three radial fuel distributions tested, the increase in fuel concentration in the center of the burner produced a slightly smaller effect on the gas temperatures near the inside wall than did the increase in the fuel concentration toward the walls. This fuel distribution also aggravated the circumferential temperature variations. The relation of these profiles to the average inside-wall temperature will be discussed in the next section.

2408

Effect of Variables on Longitudinal Profiles of

Average Inside-Wall Temperatures

Because the variations in longitudinal and circumferential temperature profiles of the inside-wall temperature were consistent, circumferential average temperatures are used in the following comparisons.

Exhaust-gas temperature. - The variations in the longitudinal profile of the average inside-wall temperature with exhaust-gas temperature level is shown in figure 16. The inside-wall temperature increases from the flame holder to the exhaust-nozzle inlet with exhaust-gas temperature level. The variation of wall temperature with exhaust-gas temperature level is slight at stations C and D because the flame has not spread to the wall. The wall temperatures at these stations are influenced more by the mass flow and inlet temperature of the cooling air than by the exhaust-gas temperature level. Downstream of station D, the wall temperature

[redacted]

increases because the temperature gradients near the wall and the radiant heat transfer increase as exhaust-gas temperature level increases. The profiles shown were obtained with a mass-flow ratio of approximately 0.145. The effect of mass-flow ratio on the wall temperature will be shown in the Combustion-Gas Mass Flow section.

Fuel distribution. - The effect of fuel distribution on the inside-wall temperatures is shown in figure 17 for an average exhaust-gas tem-
2408 perature of 3290° R and a mass-flow ratio of 0.145. The curves have been extrapolated linearly to station G, as indicated by the data of figures 16 and 18, because only two thermocouples were functioning during these readings and the temperatures at these positions were usually higher than the circumferential average temperature. Configuration B had the highest average inside-wall temperature as a result of the very high gas temperatures at the bottom of the burner; the average inside-wall temperatures of configuration A are intermediate, whereas configuration C had the lowest wall temperatures as a result of the lower gas-temperature gradients near the walls of the burner. For the two extremes in fuel distribution tested, the spread in average inside-wall temperatures at station F was 235° F, but the circumferential variations in wall temperature were greatest with configuration B.

Combustion-gas mass flow. - With an average mass-flow ratio of 0.144, the average inside-wall temperature was lowered 40° to 100° at stations F and G when the mass flow of combustion gas was decreased from 22.29 to 13.85 pounds per second (fig. 18). Comparison of the wall temperatures at the lower mass flow with wall temperatures interpolated from figure 16 indicates, however, that these reductions resulted primarily from the decrease in exhaust-gas temperature level.

Effect of Mass-Flow Ratio and Cooling-Air Temperature on Average Inside-Wall Temperatures

Mass-flow ratio. - The effect of cooling-air mass-flow ratio on the average inside-wall temperature is shown in figure 19. The limiting values of the average inside-wall temperature at stations C, D, and E with no cooling-air flow were assumed to coincide with their respective average gas temperatures 1/4 inch from the inside wall with no cooling-air flow.

As previsouly discussed, the inside-wall temperatures at stations C and D are nearly independent of the exhaust-gas temperature level and vary inversely with mass-flow ratio. The higher wall termperatures at station D result from increased radiant heat transfer from the combustion zone. Both radiant and convective heat transfer became important downstream of station D as a result of the higher gas-temperature level and the flame impingement on the walls. Thus, from station D on downstream, a distinct curve results for each tail-pipe fuel-air ratio (exhaust-gas temperature level) as shown in figure 19. Figure 19(a) shows that no cooling air is required in the first 24 inches downstream of the flame holder (station D) if the tail-pipe materials can withstand nonafterburning operation without cooling.

A mass-flow ratio of 0.12 is required in order to maintain an 2408
average inside-wall temperature of 1300° F, 48 inches downstream of the flame holder (station F) with an exhaust-gas temperature of 3825° R, and the mass-flow ratio is about 0.09 with an exhaust-gas temperature of 3435° R. An average inside-wall temperature of 1300° F, 56 inches downstream of the flame holder (station G), requires a mass-flow ratio of approximately 0.115 at 3435° R. An average inside-wall temperature of 1300° F was selected as representative in order to allow for possible hot spots as high as 1600° F.

<u>Cooling-air temperatures</u>. - The variation of inside-wall temperature with inlet cooling-air temperature (fig. 20) is similar for all exhaust-gas temperatures but differs in temperature level. The wall temperature increased with a slightly increasing rate as the cooling-air temperature was increased. When the inlet cooling-air temperature was increased 1000° F, the inside-wall temperatures increased at stations F and G about 400° F at a mass-flow ratio of 0.145. The inside-wall temperatures at station G (fig. 20(b)) were about 100° F higher than at station F (fig. 20(a)) with an exhaust-gas temperature of approximately 3060° R, and about 150° higher with an exhaust-gas temperature of 3435° R.

Interrelation of Temperatures

The interrelation of the exhaust-gas temperature, gas temperatures near the wall, inside-wall temperature, and cooling-air temperatures are shown in figure 21 for station F. The cooling-air temperature rise to station F is the vertical distance between the cooling-air temperature curve and the diagonal dashed line. This rise in cooling-air temperature becomes small as the inlet cooling air is raised to temperatures of 1500° to 1700° R, indicating that a combustion chamber with an inner liner maintains a layer of gas at approximately turbine-outlet temperature next to the outside structural wall. Consequently, the temperature of the structural wall of an insulated tail-pipe burner having an inner liner would be practically the same with or without tail-pipe burning.

The data of figure 22 can be shown to better advantage by means of the parameter $\frac{T_{g,F} - T_{w,F}}{T_{w,F} - T_{a,F}}$ which is obtained from a heat balance across the inside wall at station F. This parameter is the ratio of the over-all heat-transfer coefficients on the cooling-air and combustion-gas sides of the inside wall H_a/H_g. The ratio H_a/H_g is a function of the inlet cooling-air temperature, exhaust-gas temperature, turbine-discharge gas temperature, and mass-flow ratio for a given fuel distribution and burner geometry. This parameter can be plotted against the ratio of the inlet cooling-air temperature to the exhaust-gas temperature $T_{a,B}/T_g$ for given mass-flow ratios, turbine-discharge gas temperatures, and radial fuel distributions. Inasmuch as the cooling-air temperature $T_{a,F}$ and the effective-gas temperature $T_{g,F}$ are not generally known, and because these temperatures are functions of the same variable as the ratio H_a/H_g, the more convenient parameter $\frac{T_g - T_{w,F}}{T_{w,F} - T_{a,B}}$ is plotted in figure 22 against $\frac{T_{a,B}}{T_g}$. The parameter $\frac{T_g - T_{w,F}}{T_{w,F} - T_{a,B}}$ varies approximately linearly with $\frac{T_{a,B}}{T_g}$ but varies in level and slope with the radial fuel distribution and mass-flow ratio. The upper curve is for configuration C with a mass-flow ratio of 0.143. The second curve from the top is the mean line through the data of configuration A with mass flows of combustion gas of 22.3 and 13.8 pounds per second at a mass-flow ratio of approximately 0.143. The effect of exhaust-gas temperature level from 3064° to 3845° R is not apparent within the scatter of the data. The large discrepancy between the data points and the curve for configuration A at $\frac{T_{a,B}}{T_g} = 0.54$ amounts to only 41° R in $T_{w,F}$. The parameter $\frac{T_g - T_{w,F}}{T_{w,F} - T_{a,B}}$ is very sensitive to small changes in $T_{w,F}$ for values of $\frac{T_{a,B}}{T_g}$ greater than approximately 0.50.

The third curve is for configuration A at a mass-flow ratio of 0.098. The data of configuration C fall along the lowest curve at a mass-flow ratio of 0.143.

COOLING-AIR PRESSURE DROP

The pressure drop through the cooling passage is shown in figure 23 against the cooling-air flow. The use of σ based on inlet temperature and pressure satisfactorily correlated the data. The pressure drop increases with exhaust-gas temperature because of increased momentum pressure drop accompanying higher heat transfer to the cooling air.

The isothermal friction factor for the instrumented cooling passages is shown in figure 24. The turbulence created by the instrumentation and the interlocking stringers was great enough to make the friction factor practically independent of Reynolds number. The value was about 0.009 for a Reynolds number range of 1.6×10^4 to 1.3×10^5. Without the instrumentation the friction factor should lie closer to the line for commercial pipe. 2408

SUMMARY OF RESULTS

The effects of tail-pipe fuel-air ratio (exhaust-gas temperature level), radial distribution of tail-pipe fuel, and mass flow of combustion gas on the temperature profiles of the combustion gas and inside wall of the combustion chamber were determined for an experimental tail-pipe burner cooled by air flowing through an insulated cooling-air passage 1/2 inch in height.

Large circumferential variations existed in the combustion-gas temperature near the inside wall. These variations in combustion-gas temperature resulted in similar variations in the inside-wall temperature. The difference between the highest and the lowest gas temperatures around the circumference 1/4 inch from the inside wall was approximately 500° to 900° F, whereas the corresponding difference in the inside-wall temperatures was 400° to 600° F. These circumferential variations formed consistent patterns that were similar, although different in magnitude, for all configurations tested.

The two extremes in radial distribution of tail-pipe fuel flow, high fuel concentration toward the combustion-chamber wall and high fuel concentration in the center of the combustion chamber, produced a spread in circumferential average inside-wall temperatures of 235° F at a station 48 inches downstream of the flame holder. The configuration having a high fuel concentration toward the wall presented more of a cooling problem than is indicated by the difference in average inside-wall temperatures because the circumferential variation in temperature was greatest for this configuration.

The distance downstream of flame holders at which the flame spread to the inside wall, as determined from measurements of combustion-gas temperature near the wall, was practically unaffected by tail-pipe fuel-air ratio. However, the spread of the flame toward the wall was a function of radial fuel distribution. At no time did the flame impinge on the inside wall closer than 24 inches downstream of the flame holder. Radiant heat transfer to this section of the inside wall was insufficient as to require wall cooling in the first 24 inches if the tail-pipe materials could withstand nonafterburning operation without cooling.

With the most uniform distribution of tail-pipe fuel tested and an inlet cooling-air temperature of 520° R, an average inside-wall temperature of 1300° F at a station 48 inches downstream of the flame holder required mass-flow ratios of 0.12 and 0.09 at exhaust-gas temperatures of 3825° and 3435° R, respectively. Increasing the distance to 56 inches downstream of the flame holder necessitated a mass-flow ratio of 0.115 with an exhaust-gas temperature of 3435° R.

2408

At a mass-flow ratio of 0.145, the inside-wall temperatures at a station 48 inches downstream of the flame holder were increased approximately 4/10° per degree increase in inlet cooling-air temperature.

It was shown that the temperature of the structural wall of an insulated tail-pipe burner having an inner liner would be practically the same with or without tail-pipe burning.

Lewis Flight Propulsion Laboratory
National Advisory Committee for Aeronautics
Cleveland, Ohio.

APPENDIX A

CALCULATION OF EXHAUST-GAS TEMPERATURE

The exhaust-gas temperature was calculated from the following equation when the nozzle was choked:

$$T_g = \gamma_g \frac{(\gamma_g + 1)}{2} \frac{g}{R} \left(\frac{p_n C_n C_T A_n}{W_g}\right)^2 \tag{B1}$$

where $C_n = 0.965$.

$$C_T = \left[1 + 9\times10^{-6} (t_n - 70)\right]^2$$

and p_n was obtained from the critical pressure ratio corresponding to γ_g

$$p_n = P_n \left(\frac{\gamma_g + 1}{2}\right)^{\frac{\gamma_g}{\gamma_g - 1}}$$

When the nozzle was unchoked

$$T_g = \frac{(\gamma_g - 1)}{\gamma_g W_g^2} \frac{g}{2R} \frac{1}{\left[1 - \left(\frac{p_0}{P_n}\right)^{\frac{\gamma_g - 1}{\gamma_g}}\right]} \left(\frac{F_j}{C_j}\right) \tag{B2}$$

where $C_j = 0.97$.

2408

APPENDIX B

SYMBOLS

A_n area of exhaust-nozzle throat at 70° F, sq ft

C_j ratio of scale jet thrust to ideal jet thrust

C_n exhaust-nozzle flow coefficient

C_T area thermal expansion coefficient

D_h hydraulic diameter of cooling passage (twice cooling passage height), ft

F_j scale jet thrust, lb

f isothermal friction factor

f/a fuel-air ratio

$(f/a)_t$ tail-pipe fuel-air ratio

g acceleration due to gravity, ft/sec^2

H_a combined coefficient of heat transfer on the cooling-air side, Btu/(hr)(sq ft)(°R)

H_g combined coefficient of heat transfer on combustion-gas side, Btu/(hr)(sq ft)(°R)

l flow distance between stations B and F, ft

P_n total pressure at exhaust-nozzle throat, lb/sq ft abs.

P_5 turbine-outlet total pressure, lb/sq ft abs.

P_8 exhaust-nozzle total pressure, lb/sq ft abs.

p_0 static pressure in tunnel test section, lb/sq ft abs.

p_n static pressure at exhaust-nozzle throat, lb/sq ft abs.

$\bar{q}$ average dynamic pressure between stations B and F, lb/sq ft

R gas constant, ft-lb/(lb)(°R)

Re Reynolds number

[redacted]

T_a cooling-air temperature, $^{\circ}R$ or $^{\circ}F$

T_g exhaust-gas temperature at nozzle exit, $^{\circ}R$

$T_{g,1/4}$ combustion-gas temperature measured 1/4 inch from inside wall, $^{\circ}R$ or $^{\circ}F$

$T_{g,1/2}$ combustion-gas temperature measured 1/2 inch from inside wall, $^{\circ}R$ or $^{\circ}F$

T_s outside-wall temperature, $^{\circ}F$ 2408

T_s' turbine-outlet total temperature, $^{\circ}R$

T_w inside-wall temperature, $^{\circ}R$ or $^{\circ}F$

T_1 engine-inlet total temperature, $^{\circ}R$

t_n average temperature of exhaust nozzle lip, $^{\circ}F$

W_a cooling-air flow, lb/sec

$W_{f,e}$ engine fuel flow, lb/hr

$W_{f,t}$ tail-pipe fuel flow, lb/hr

W_g combustion gas flow, lb/sec

W_a/W_g mass-flow ratio

γ_g ratio of specific heats of exhaust gas corresponding to total fuel-air ratio and exhaust-gas temperature

$\eta_{b,t}$ tail-pipe combustion efficiency

σ ratio of density at prevailing temperature and pressure to density at standard temperature and pressure

Subscripts:

B to G longitudinal stations

REFERENCES

1. Koffel, William K., Stamper, Eugene, and Sanders, Newell D.: Cooling of Ram Jets and Tail-Pipe Burners - Analytical Method for Determining Temperatures of Combustion Chamber Having Annular Cooling Passage. NACA RM E9L09, 1950.

[redacted]

2. Conrad, E. William, and Jansen, Emmert T.: Effects of Internal Configurations on Afterburner Shell Temperatures. NACA RM E51I07

3. Wallner, Lewis E., and Jansen, Emmert T.: Full-Scale Investigation of Cooling Shroud and Ejector Nozzle for a Turbojet Engine - Afterburner Installation. NACA RM E51J04

4. Sibulkin, Merwin, and Koffel, William K.: Chart for Simplifying Calculations of Pressure Drop of a High-Speed Compressible Fluid under Simultaneous Action of Friction and Heat Transfer - Application to Combustion-Chamber Cooling Passages. NACA TN 2067, 1950.

5. Fiock, Ernest F., and Dahl, Andrew I.: Sixteenth Monthly Report of Progress on the Development of Thermocouple Pyrometers for Gas Turbines. Nat. Bur. Standards. April 14, 1947.

6. Blackshear, Perry L., Jr.: Sonic-Flow-Orifice Temperature Probe for High-Gas-Temperature Measurements. NACA TN 2167, 1950.

2408

TABLE I. - OPERATING CONDITIONS

Run	Altitude (ft)	Exhaust-nozzle exit area (sq ft)	Flight Mach number M_0	Ambient pressure p_0 $\left(\frac{lb}{sq\ ft\ abs.}\right)$	Engine-inlet total pressure P_2 $\left(\frac{lb}{sq\ ft\ abs.}\right)$	Engine-inlet total temperature T_1 (°R)	Cooling-air inlet temperature T_a (°R)	Engine fuel flow $W_{f,e}$ $\left(\frac{lb}{hr}\right)$	Tail-pipe fuel flow $W_{f,t}$ $\left(\frac{lb}{hr}\right)$	Engine air flow W_a $\left(\frac{lb}{sec}\right)$	Total fuel-air ratio $\left(\frac{f}{a}\right)$	Tail-pipe fuel-air ratio $\left(\frac{f}{a}\right)_t$	Mass ratio $\frac{W_a}{W_g}$	Tail-pipe combustion efficiency $\eta_{b,t}$	Turbine-outlet total pressure P_5 $\left(\frac{lb}{sq\ ft\ abs.}\right)$	Turbine-outlet total temperature T_5' (°R)	Exhaust-nozzle total pressure P_8 $\left(\frac{lb}{sq\ ft\ abs.}\right)$	Exhaust-gas total temperature T_8 (°R)	Run
CONFIGURATION A																			
1	30,000	1.846	0.512	633	757	506	541	1194	1885	21.03	0.0407	0.0325	0.0672	0.939	1373	1640	1272	2994	1
2			.520	629	755	506	530	1186	1845	21.14	.0398	.0315	.0814	.871	1350	1632	1248	2858	2
3			.521	627	753	494	526	1268	2090	21.93	.0425	.0345	.1006	.883	1432	1630	1327	2993	3
4			.549	620	761	501	518	1204	1855	21.40	.0397	.0313	.1029	.902	1361	1627	1271	2891	4
5			.516	627	751	508	522	1194	1850	20.83	.0316	.0323	.1033	.945	1361	1646	1261	2996	5
6			.522	626	753	506	518	1190	1850	21.08	.0374	.0318	.1218	.919	1363	1637	1261	2934	6
7			.511	630	753	497	518	1263	2030	21.19	.0432	.0347	.0986	.945	1413	1636	1313	3117	7
8			.521	627	754	504	536	1235	1960	-----	------	------	a.0949	-----	----	1622	----	----	8
9			.514	629	753	503	635	1222	1970	20.99	.0422	.0339	.0960	.965	1397	1621	1296	3106	9
10			.516	627	753	503	835	1221	1955	21.05	.0419	.0335	.1002	.964	1396	1630	1296	3085	10
11			.512	629	753	503	942	1230	1955	20.99	.0422	.0336	.0968	.969	1400	1627	1298	3110	11
12			.519	626	753	503	948	1225	1955	21.06	.0419	.0335	.0965	.959	1396	1622	1296	3081	12
13			.511	626	748	497	965	1239	2005	21.13	.0426	.0344	.0948	.955	1408	1632	1307	3110	13
14			.510	628	750	508	1037	1225	1955	20.86	.0423	.0339	.0960	.967	1393	1629	1293	3121	14
15			.507	631	752	508	1115	1228	1950	20.86	.0423	.0338	.0988	.979	1395	1633	1295	3133	15
16			.512	629	753	507	1245	1231	1950	21.05	.0420	.0335	.0984	.944	1393	1630	1292	3063	16
17			.510	629	751	506	1343	1232	1935	21.11	.0417	.0332	.0985	.942	1392	1632	1291	3045	17
18			.506	632	753	506	1413	1211	1930	20.95	.0416	.0332	.1016	.976	1392	1622	1291	3094	18
19			.524	628	757	499	494	909	0	22.92	.0110	.0110	.0959	-----	989	1185	888	----	19
20			.518	629	756	503	500	907	0	21.23	.0119	.0119	.0997	-----	989	1188	886	----	20
21			.515	631	756	503	508	980	1485	21.66	.0316	.0228	.1012	.304	1136	1330	1043	1706	21
22			.514	633	758	504	510	1075	1815	21.48	.0374	.0290	.1005	.645	1259	1451	1162	2389	22
23			.511	631	754	506	525	1151	1975	21.41	.0406	.0326	.1041	.756	1338	1551	1235	2702	23
24			.509	631	752	506	525	1170	2015	21.28	.0416	.0336	.1029	.779	1346	1570	1244	2787	24
25			.509	631	753	514	555	1233	2019	20.84	.0433	.0350	.0662	.938	1392	1641	1291	3121	25
26			.514	629	753	503	546	1244	2032	21.13	.0431	.0347	.0694	.924	1404	1632	1302	3088	26
27			.514	629	753	503	529	1248	1998	21.13	.0427	.0341	.0985	.948	1410	1624	1306	3102	27
28			.519	627	753	499	529	1268	2085	21.46	.0434	.0352	.1206	.900	1421	1638	1317	3059	28
29			.509	631	753	503	517	1268	2079	21.13	.0440	.0356	.1519	.941	1422	1636	1317	3152	29
30			.506	639	761	503	507	1268	2079	21.35	.0435	.0352	.1872	.922	1426	1632	1323	3102	30
31			.514	631	755	520	541	1221	1988	20.78	.0429	.0346	.1467	.916	1380	1648	1278	3076	31
32			.514	631	755	511	657	1200	1988	21.03	.0422	.0344	.1482	.963	1400	1634	1299	3101	32
33			.518	629	755	504	750	1183	2028	21.24	.0420	.0345	.1435	.943	1406	1632	1305	3065	33
34			.516	629	754	508	850	1166	2045	21.06	.0424	.0351	.1447	.957	1407	1637	1303	3104	34
35			.520	629	756	503	1028	1224	1988	21.30	.0419	.0377	.1426	.949	1412	1626	1310	3067	35
36			.522	627	755	505	1133	1221	1988	21.39	.0417	.0335	.1438	.936	1412	1624	1310	3040	36
37			.511	636	760	501	1335	1220	1988	21.54	.0414	.0333	.1410	.945	1421	1620	1317	3028	37
38			.520	630	757	506	1462	1226	1978	21.34	.0417	.0334	.1391	.956	1415	1626	1313	3068	38
39			.521	631	759	506	1587	1230	1978	21.42	.0416	.0333	.1417	.938	1415	1632	1312	3040	39
40			.519	628	754	506	509	889	0	21.17	.0117	.0117	.1040	-----	993	1202	890	----	40
41			.515	627	751	500	1355	819	1615	21.37	.0316	.0253	.1453	.372	1165	1358	1064	1805	41
42			.516	627	752	503	1550	974	2005	21.27	.0389	.0332	.1413	.836	1339	1548	1237	2752	42
43			.514	631	755	508	1650	1217	1942	21.16	.0415	.0331	.1439	.960	1404	1631	1302	3067	43
44	30,000	1.903	0.516	628	753	504	519	1262	2360	21.28	0.0473	0.0401	0.1216	0.888	----	1634	1303	3215	44
45			.499	634	751	506	513	1262	2360	20.94	.0480	.0409	.1444	.927	----	1640	1304	3317	45
46			.510	629	751	506	513	1265	2255	20.94	.0467	.0392	.1688	-----	----	1649	----	----	46
47			.511	630	753	508	513	1268	2260	21.03	.0466	.0391	.1917	.935	----	1647	1299	3266	47
48			.509	628	749	508	514	1248	2227	20.77	.0465	.0387	.1481	.981	1403	1627	1296	3341	48

[redacted]

2408

49	30,000	1.903	0.515	631	756	501	726	1243	2217	21.34	0.0450	0.0374	0.1420	0.928	1408	1617	1298	3175	49
50			.520	625	751	499	839	1253	2239	21.32	.0455	.0379	.1398	.923	1408	1622	1298	3189	50
51			.515	627	751	501	915	1243	2186	21.22	.0499	.0372	.1441	.948	1405	1624	1296	3207	51
52			.514	628	752	503	1013	1224	2186	21.12	.0448	.0374	.1443	.970	1406	1622	1297	3237	52
53			.516	629	754	503	1117	1221	2186	21.23	.0446	.0371	.1427	.957	1403	1613	1295	3204	53
54			.521	627	754	505	1222	1235	2186	21.13	.0450	.0373	.1424	.950	1400	1616	1393	3214	54
55			.518	630	756	508	500	890	0	22.54	.0117	.0117	.1039	-----	981	1188	878	----	55
56			.520	629	756	506	509	932	1290	22.49	.0291	.0198	.1048	.094	1066	1260	957	1352	56
57			-----	630	---	499	500	1002	1595	-----	------	------	a.1033	-----	1164	1347	1053	----	57
58			.509	631	753	504	509	1068	1840	22.45	.0382	.0299	.1026	.490	1249	1451	1139	2180	58
59			-----	629	---	510	512	1046	1770	-----	------	------	a.1033	-----	1221	1442	1111	----	59
60			.505	633	753	505	515	1142	1855	22.47	.0396	.0310	.1025	.916	1321	1532	1215	2904	60
61			.521	632	760	505	500	1171	2050	22.47	.0417	.0334	.1002	.829	1327	1523	1234	2862	61
62	30,000	1.980	0.511	632	755	507	533	1236	2620	20.87	0.0513	0.0453	0.0953	0.953	1400	1630	1290	3516	62
63			.509	631	753	506	530	1247	2660	21.00	.0517	.0459	.1050	.930	1405	1640	1294	3484	63
64			.518	631	757	504	526	1247	2615	21.24	.0505	.0444	.1071	.936	1410	1627	1299	3443	64
65			.516	629	754	503	528	1250	2610	21.17	.0506	.0446	.1326	.945	1411	1636	1300	3470	65
66			-----	629	---	---	530	1220	2550	-----	------	------	a.1430	-----	1388	1621	1279	----	66
67			.520	629	756	497	518	1250	2620	21.36	.0503	.0443	.1524	.931	1414	1625	1303	3422	67
68			-----	629	---	---	519	1241	2545	-----	------	------	a.1671	-----	1393	1636	1282	----	68
69			.520	629	756	503	513	1260	2600	21.30	.0503	.0441	.1699	.923	1409	1625	1297	3408	69
70			.524	629	758	503	502	1259	2590	21.43	.0499	.0436	.1796	.929	1415	1620	1302	3401	70
71			.512	632	756	512	1046	1227	2600	20.87	.0509	.0451	.1571	.932	1395	1637	1283	3457	71
72			.521	627	754	513	1059	1212	2610	20.88	.0509	.0453	.1711	.918	1391	1648	1278	3427	72
73			.516	629	754	504	1050	1240	2620	21.22	.0505	.0447	.1715	.910	1410	1637	1293	3394	73
74			.522	624	751	498	493	889	0	21.41	.0115	.0115	.0992	-----	964	1182	850	----	74
75			.519	628	754	505	511	915	1395	21.13	.0304	.0215	.0974	.102	1040	1241	933	1353	75
76			.518	629	755	509	520	939	1520	21.00	.0325	.0239	.1010	.273	1094	1302	987	1659	76
77			.512	627	750	500	502	987	1645	21.27	.0344	.0258	.1000	.388	1147	1342	1041	1880	77
78			.511	631	754	500	507	1078	2000	21.30	.0401	.0323	.0966	.798	1260	1455	1150	2737	78
79			.512	632	756	503	512	1163	2150	21.30	.0432	.0356	.1008	.935	1335	1555	1226	3108	79
80			.524	629	758	507	530	1240	2710	21.10	.0520	.0465	.1000	.906	1405	1636	1294	3449	80
81			.521	625	752	505	520	1233	2592	21.23	.0501	.0441	.1436	.923	1401	1626	1289	3394	81
82			.507	630	751	505	659	1223	2600	20.96	.0507	.0448	.1480	.952	1401	1631	1289	3481	82
83			.518	624	749	507	771	1213	2612	20.96	.0507	.0450	.1411	.921	1394	1632	1283	3425	83
84			-----	629	---	---	898	1261	2664	-----	------	------	a.1608	-----	1400	1637	1285	----	84
85			.512	626	749	504	1049	1236	2628	21.02	.0510	.0452	.1578	.931	1402	1631	1289	3454	85
86			.522	624	751	503	1135	1228	2621	21.17	.0505	.0446	.1428	.912	1398	1627	1286	3393	86
87			-----	625	---	---	1229	1368	2628	-----	------	------	a.1442	-----	1399	1632	1287	----	87
88			.511	631	756	506	1309	1402	2628	21.18	.0528	.0449	.1430	.909	1406	1631	1291	3402	88
89			.510	629	751	499	1408	1251	2612	21.26	.0505	.0444	.1412	.919	1409	1625	1295	3403	89
90	40,000	1.980	b0.515	392	471	503	548	828	1411	13.16	0.0473	0.0385	0.1415	0.921	853	1621	782	3272	90
91				392	473	504	528	804	1341	13.25	.0459	.0365	.1451	.979	859	1620	791	3284	91
92				393	473	505	720	822	1264	13.23	.0434	.0343	.1440	1.026	854	1607	786	3262	92
93				392	472	505	837	831	1269	13.26	.0438	.0344	.1415	1.013	855	1612	786	3258	93
94				393	470	501	1013	820	1292	13.16	.0446	.0353	.1438	.970	848	1608	778	3223	94
95				394	471	506	1154	817	1306	13.03	.0453	.0361	.1459	.983	848	1615	778	3281	95
96				389	469	500	1210	831	1273	13.23	.0442	.0347	.1366	.994	854	1611	785	3244	96
97				392	469	504	1340	829	1306	12.99	.0457	.0363	.1418	.986	847	1617	779	3306	97
98	30,000	2.16	0.514	636	761	501	523	1268	3865	21.57	0.0661	0.0650	0.1374	0.825	1427	1637	1302	3811	98
99			.516	634	760	504	520	1273	3870	21.47	.0666	.0653	.1651	.820	1427	1642	1299	3817	99
100			.515	631	756	506	515	1258	3870	21.24	.0670	.0660	.1871	.823	1415	1642	1291	3845	100
101			.518	634	761	503	508	1087	2295	21.52	.0437	.0367	.1906	-----	1269	1458	1147	----	101
102			.511	630	753	500	510	1177	2850	21.44	.0522	.0470	.1884	.924	1340	1552	1218	3480	102

[a]Based on average W_g.

[b]Approximately 0.515.

NACA

TABLE I. - OPERATING CONDITIONS - Concluded

Run	Altitude (ft)	Exhaust nozzle exit area (sq ft)	Flight Mach number M_0	Ambient pressure p_0 $\left(\frac{lb}{sq\ ft\ abs.}\right)$	Engine-inlet total pressure P_2 $\left(\frac{lb}{sq\ ft\ abs.}\right)$	Engine-inlet total temperature T_1 (°R)	Cooling-air inlet temperature T_a (°R)	Engine fuel flow $W_{f,e}$ $\left(\frac{lb}{hr}\right)$	Tail-pipe fuel flow $W_{f,t}$ $\left(\frac{lb}{hr}\right)$	Engine air flow W_a $\left(\frac{lb}{sec}\right)$	Total fuel-air ratio $\left(\frac{f}{a}\right)$	Tail-pipe fuel-air ratio $\left(\frac{f}{a}\right)_t$	Mass ratio $\frac{W_a}{W_g}$	Tail-pipe combustion efficiency $\eta_{b,t}$	Turbine-outlet total pressure P_5 $\left(\frac{lb}{sq\ ft\ abs.}\right)$	Turbine-outlet total temperature T_8' (°R)	Exhaust-nozzle total pressure P_8 $\left(\frac{lb}{sq\ ft\ abs.}\right)$	Exhaust-gas total temperature T_g (°R)	Run
CONFIGURATION B																			
1	30,000	1.903	0.511	630	753	503	507	1255	2359	21.14	0.0475	0.0402	0.0985	0.904	1406	1619	1300	3248	1
2			.524	625	754	501	507	1260	2355	21.45	.0468	.0396	.1198	.873	1409	1623	1301	3161	2
3			.519	627	753	507	500	1282	2345	21.22	.0475	.0399	.1422	.885	1410	1631	1298	3215	3
4			.514	629	753	504	500	1279	2373	21.28	.0477	.0403	.1691	.890	1414	1636	1305	3232	4
5			.516	628	753	501	500	1258	2355	21.42	.0469	.0397	.1891	.860	1404	1622	1296	3140	5
6			.514	628	752	504	495	1266	2373	21.01	.0481	.0409	.1449	.921	1416	1633	1306	3305	6
7			.524	628	757	505	748	1236	2342	21.29	.0467	.0397	.1417	.894	1411	1625	1301	3197	7
8			.511	631	754	503	737	1243	2345	21.17	.0471	.0400	.1452	.937	1422	1628	1311	3289	8
9			.514	629	753	504	838	1251	2345	21.04	.0475	.0392	.1460	-----	1421	1633	----	----	9
10			.512	629	752	507	938	1250	2337	20.94	.0476	.0403	.1457	.921	1408	1630	1299	3285	10
11			.525	629	759	505	1038	1158	2423	21.42	.0464	.0408	.1412	.878	1409	1623	1298	3156	11
12			.514	630	754	507	1127	1129	2438	21.08	.0470	.0416	.1425	.893	1395	1617	1289	3208	12
13			.512	628	751	501	1223	1115	2459	21.22	.0468	.0418	.1425	.875	1399	1622	1289	3164	13
CONFIGURATION C																			
1	30,000	1.903	0.512	632	756	505	524	1251	2190	21.26	0.0450	0.0372	0.1472	0.972	1412	1625	1306	3248	1
2			.507	634	756	500	723	1258	2210	21.43	.0450	.0370	.1419	.957	1420	1627	1312	3220	2
3			.515	627	751	495	828	1259	2195	21.39	.0449	.0372	.1426	.955	1415	1624	1308	3214	3
4			.510	629	751	501	925	1257	2195	21.28	.0451	.0370	.1438	.965	1412	1623	1307	3237	4
5			.504	624	754	498	1040	1244	2190	21.34	.0447	.0372	.1389	.980	1419	1622	1313	3251	5
6			.512	632	756	505	1233	1385	2190	21.33	.0465	.0371	.1416	.975	1417	1631	1312	3245	6
7			.510	633	756	500	1450	1424	2180	21.36	.0469	.0373	.1418	.980	1417	1628	1312	3237	7
8	30,000	2.16	0.510	634	757	508	524	1205	4365	20.84	0.0743	0.0752	0.1912	0.715	1389	1611	1266	3764	8

2408

TABLE II - CIRCUMFERENTIAL AVERAGE TEMPERATURES, ^{o}F

Run	Station C					Station D					Station E					Station F					Run
	Combustion gas		Inside wall	Outside wall	Cooling air	Combustion gas		Inside wall	Outside wall	Cooling air	Combustion gas		Inside wall	Outside wall	Cooling air	Combustion gas		Inside wall	Outside wall	Cooling air	
	$T_{g,1/2}$	$T_{g,1/4}$	T_w	T_s	T_a	$T_{g,1/2}$	$T_{g,1/4}$	T_w	T_s	T_a	$T_{g,1/2}$	$T_{g,1/4}$	T_w	T_s	T_a	$T_{g,1/2}$	$T_{g,1/4}$	T_w	T_s	T_a	
	CONFIGURATION A																				
1	1098	1093	711	125	110	1317	1127	843	229	204	1567	1410	963	325	291	1819	1683	1198	469	393	1
2	1085	1099	661	100	93	1290	1110	780	183	174	1530	1368	884	258	245	1818	1625	1107	403	330	2
3	1100	1087	600	78	84	1342	1145	708	137	148	1696	1449	822	198	207	2113	1856	1020	305	268	3
4	1082	1079	600	75	73	1273	1107	706	133	144	1517	1359	799	193	201	1764	1576	949	308	269	4
5	1091	1098	612	82	81	1305	1103	726	150	153	1561	1397	828	214	215	1815	1629	1046	339	290	5
6	1083	1090	564	73	75	1292	1090	663	124	139	1525	1367	759	176	188	1805	1607	962	281	252	6
7	1103	1076	631	72	70	1310	1114	699	128	141	1684	1436	817	188	186	2007	1756	1059	313	289	7
8	1095	1074	666	100	92	1286	1111	749	173	170	1611	1445	892	253	227	1951	1767	1032	399	346	8
9	1096	1079	691	202	191	1299	1120	768	285	252	1632	1448	912	356	312	1968	1774	1038	502	415	9
10	1103	1079	773	392	388	1292	1125	834	436	441	1645	1456	966	494	448	1956	1777	1090	610	558	10
11	1089	1099	828	489	492	1298	1119	884	520	535	1673	1490	1015	573	572	1979	1795	1137	685	639	11
12	1097	1079	832	498	500	1303	1131	888	527	544	1649	1480	1011	577	581	1972	1805	1134	686	644	12
13	1102	1062	831	508	514	1282	1109	882	536	554	1655	1452	1011	581	588	1981	1776	1143	680	650	13
14	1119	1100	863	582	583	1324	1169	916	591	606	1681	1499	1044	638	640	1997	1824	1168	735	701	14
15	1130	1110	915	651	662	1311	1198	963	666	645	1702	1511	1085	707	720	2011	1835	1201	791	771	15
16	1134	1118	983	773	788	1346	1188	1032	782	812	1727	1538	1147	820	829	2022	1856	1256	899	876	16
17	1137	1146	1042	872	887	1327	1217	1090	869	910	1778	1611	1203	907	918	2043	1877	1302	977	958	17
18	1130	1138	1075	939	956	1314	1210	1122	932	972	1722	1532	1229	968	978	1987	1869	1364	1028	1012	18
19	721	667	328	37	38	----	----	363	54	74	----	----	366	71	101	----	----	365	93	112	19
20	704	651	348	44	43	----	----	368	61	80	----	----	370	83	104	----	----	371	112	122	20
21	847	817	406	50	52	----	----	460	77	98	1051	----	469	103	134	1105	1065	514	145	155	21
22	956	920	469	59	62	----	----	541	97	114	1216	----	573	131	160	1304	1266	661	189	191	22
23	1046	1025	521	73	77	1127	1051	623	124	139	1355	1143	681	173	198	1638	1445	799	250	245	23
24	1063	1048	534	71	76	1149	1061	647	120	133	1404	1185	701	168	195	1775	1533	830	244	247	24
25	1129	1092	792	131	123	1324	1139	889	262	227	1657	1436	1057	357	310	2111	1865	1226	535	438	25
26	1085	1085	772	114	116	1318	1135	863	214	207	1650	1411	1026	310	286	2093	1841	1189	473	378	26
27	1094	1077	684	90	92	1308	1122	774	165	173	1612	1386	918	246	238	1962	1783	1046	376	329	27
28	1110	1091	643	82	90	1329	1138	731	136	156	1694	1436	872	207	214	1982	1845	1023	335	296	28
29	1064	1079	582	71	73	1328	1128	657	114	135	1677	1443	788	157	190	2014	1820	912	286	253	29
30	1077	1062	520	57	61	1299	1119	588	88	116	1635	1348	697	126	159	1985	1770	837	224	206	30
31	1144	1130	607	123	102	1365	1170	701	198	172	1682	1509	834	246	244	1682	1509	967	370	315	31
32	1101	1080	640	213	210	1315	1125	697	256	269	1619	1397	842	293	312	1956	1781	966	392	378	32
33	1103	1082	681	296	305	1308	1136	758	339	358	1624	1411	858	380	396	1953	1791	999	467	454	33
34	1098	1090	751	378	399	1311	1110	805	413	442	1635	1451	921	452	472	2000	1817	1084	551	523	34
35	1079	1064	850	564	573	1295	1106	896	579	610	1641	1350	1001	616	633	1965	1801	1155	678	676	35
36	1102	1078	906	662	674	1303	1120	949	664	705	1625	1394	1054	704	723	2055	1807	1166	757	758	36
37	1110	1077	1024	842	871	1310	1139	1063	848	892	1639	1420	1159	874	895	2071	1833	1253	920	920	37
38	1160	1111	1109	985	1000	1308	1169	1148	979	1017	1694	1460	1241	1003	1017	2099	1884	1327	1045	1041	38
39	1131	1107	1188	1108	1132	1339	1210	1226	1100	1138	1687	1474	1314	1119	1131	2106	1917	1394	1155	1152	39
40	706	670	347	52	53	----	----	362	72	87	----	----	366	125	118	----	----	390	135	137	40
41	902	862	912	864	893	----	----	913	838	888	----	1001	922	835	868	1070	1067	923	838	864	41
42	1088	1085	1123	1069	1069	1119	1071	1143	1049	1105	1361	1244	1188	1059	1080	1595	1459	1232	1077	1090	42
43	1142	1138	1234	1171	1189	1373	1200	1269	1161	1195	1712	1535	1356	1182	1188	2126	1936	1429	1217	1209	43
44	1100	1067	620	77	76	1302	1066	698	133	153	1727	1479	1479	856	198	208	2255	1966	1032	308	44
45	1102	1062	583	72	73	1296	1060	656	117	141	1734	1502	808	169	190	2252	1970	922	274	265	45
46	1106	1061	545	69	70	1305	1065	616	105	132	1711	1528	758	149	177	2102	1909	903	244	239	46
47	1100	1048	513	65	67	1308	1071	583	95	122	1720	1497	653	135	163	2119	1894	866	211	220	47
48	1098	1073	584	78	74	1342	1089	667	132	147	1737	1492	818	171	204	2170	1895	945	255	274	48

[redacted]

49	1083	1071	682	290	282	1324	1080	749	327	341	1710	1473	877	371	385	2138	1856	1026	488	448	49
50	1093	1062	744	384	390	1336	1072	803	409	435	1736	1476	921	451	471	2161	1877	1085	555	525	50
51	1093	1061	794	470	464	1328	1073	844	491	523	1713	1454	972	549	553	2209	1854	1095	627	601	51
52	1099	1069	860	563	563	1323	1084	897	576	612	1726	1474	1020	627	635	2236	1884	1137	703	679	52
53	1100	1073	901	652	662	1326	1093	947	665	697	1728	1477	1065	702	715	2150	1903	1177	779	754	53
54	1113	1091	967	754	765	1349	1110	1009	753	793	1751	1628	1085	797	810	2181	1906	1230	870	845	54
55	690	596	337	52	52	----	----	358	77	97	----	----	365	105	117	----	----	375	151	150	55
56	760	662	385	58	58	----	----	420	90	111	----	----	440	124	137	----	----	466	174	175	56
57	842	738	444	60	63	----	----	487	100	122	----	----	527	141	153	1184	1053	582	196	202	57
58	937	837	513	70	69	----	----	565	119	138	1114	1055	618	173	181	1216	1143	706	246	246	58
59	933	831	501	69	69	----	----	554	115	135	1073	1001	617	165	174	1160	1118	685	229	235	59
60	1038	973	590	79	76	1147	----	670	134	153	1405	1237	732	194	202	1795	1438	917	286	278	60
61	1029	933	560	70	69	1062	----	640	131	150	1313	1164	735	178	192	1682	1451	865	276	270	61
62	1114	1085	720	102	96	1421	1174	829	189	189	2098	1734	998	292	268	2504	2263	1257	507	393	62
63	1099	1089	683	88	86	1356	1124	783	165	169	1988	1714	986	261	230	2342	2166	1233	451	371	63
64	1085	1101	681	90	88	1420	1174	790	160	173	1950	1667	965	245	240	2487	2148	1187	424	350	64
65	1102	1088	634	81	81	1412	1164	722	133	153	2003	1657	889	197	209	2391	2134	1064	330	301	65
66	1086	1061	580	91	88	1336	1126	638	130	151	1885	1690	836	188	205	2299	2072	1017	307	281	66
67	1104	1083	581	74	75	1381	1144	671	116	141	1968	1630	831	168	191	2289	2084	999	283	271	67
68	1090	1070	544	77	79	1341	1117	598	111	135	1907	1689	768	158	182	2294	2073	957	259	248	68
69	1099	1066	555	69	70	1365	1124	635	106	132	1878	1644	784	152	178	2263	2104	950	260	250	69
70	1094	1060	529	59	60	1330	1139	604	90	118	1824	1593	739	132	161	2220	1972	914	235	228	70
71	1105	1120	866	592	594	1459	1204	922	610	632	2028	1735	1072	654	658	2447	2243	1243	728	716	71
72	1133	1121	870	595	606	1496	1218	928	616	642	2013	1801	1071	658	667	2473	2265	1238	726	719	72
73	1116	1087	854	591	598	1443	1165	904	603	632	2013	1718	1035	639	653	2369	2217	1219	712	700	73
74	716	663	342	38	38	----	----	346	57	79	----	----	355	79	102	----	----	370	107	121	74
75	757	----	400	62	62	----	----	433	91	109	----	----	449	120	140	----	----	477	160	169	75
76	832	----	438	69	70	1057	----	477	102	119	----	----	502	135	155	1109	1025	546	188	192	76
77	862	----	453	52	53	----	----	500	85	106	1056	----	541	118	143	1208	1126	536	169	184	77
78	959	640	527	62	63	1026	----	593	102	125	1263	1128	672	146	171	1529	1297	781	223	234	78
79	1053	1066	626	77	75	1220	1088	719	129	148	1593	1305	847	189	206	2040	1677	1015	298	288	79
80	1114	1095	701	96	93	1482	1183	821	171	180	2073	1750	1010	271	264	2545	2235	1228	465	402	80
81	1101	1085	595	79	79	1471	1159	692	124	144	1831	1660	865	193	199	2394	2145	1063	307	287	81
82	1099	1101	862	210	218	1502	1178	745	266	280	1916	1698	914	318	329	2409	2174	1102	428	409	82
83	1119	1109	726	335	328	1520	1194	803	369	384	1952	1719	972	420	443	2417	2188	1158	528	516	83
84	1120	1090	776	428	450	1562	1203	841	440	492	2076	1795	1002	480	514	2420	2200	1178	580	572	84
85	1115	1115	860	582	594	1517	1206	913	599	630	2004	1759	1065	643	653	2427	2223	1203	717	708	85
86	1102	1124	918	662	680	1563	1178	977	674	713	2058	1781	1128	719	732	2450	2234	1256	801	783	86
87	1114	1133	973	757	774	1589	1250	1031	763	803	2126	1872	1198	812	819	2466	2263	1346	884	870	87
88	1147	1106	1027	840	851	1508	1178	1077	842	871	2005	1775	1210	885	887	2460	2240	1366	964	935	88
89	1110	1115	1088	931	950	1525	1212	1136	930	964	2019	1771	1281	965	976	2459	2261	1401	1044	1014	89
90	1045	1017	643	181	113	1136	1017	719	289	204	1610	1213	870	366	296	2176	1787	1065	473	389	90
91	1052	1025	618	118	90	1165	1043	704	189	169	1625	1255	852	246	244	2166	1800	1022	355	327	91
92	1039	1013	691	292	276	1154	1024	753	338	339	1578	1228	878	391	387	2094	1740	1027	475	468	92
93	1045	1015	754	409	391	1164	1027	805	452	449	1597	1263	936	509	499	2126	1822	1081	594	566	93
94	1046	1002	845	559	561	1153	1025	892	582	604	1636	1265	1002	624	633	2148	1832	1139	694	681	94
95	1052	1011	926	701	699	1159	1004	972	710	733	1652	1269	1091	744	755	2179	1822	1220	818	804	95
96	1040	1022	955	724	750	1178	1038	994	714	768	1709	1310	1088	741	783	2240	1924	1215	786	797	96
97	1067	1017	1054	884	922	1174	1048	1091	862	931	1680	1293	1181	881	938	2163	1841	1293	931	959	97
98	1083	1068	597	77	78	1737	1179	707	127	145	2610	2330	1018	199	231	2865	2705	1191	364	324	98
99	1080	1081	556	69	73	1748	1167	653	112	133	2617	2300	943	180	201	2840	2677	1121	333	288	99
100	1078	1074	525	67	69	1690	1167	613	100	123	2613	2275	902	151	183	2844	2653	1049	292	257	100
101	947	853	422	51	56	1094	1120	479	77	99	1324	1135	574	99	131	1778	1234	690	166	171	101
102	1031	990	449	57	60	1203	1189	524	86	106	1711	1452	657	120	143	2307	1907	825	214	200	102

NACA

2408

TABLE II - CIRCUMFERENTIAL AVERAGE TEMPERATURES, ^{o}F - Concluded

Run	Station C					Station D					Station E					Station F					Run
	Combustion gas		Inside wall	Outside wall	Cooling air	Combustion gas		Inside wall	Outside wall	Cooling air	Combustion gas		Inside wall	Outside wall	Cooling air	Combustion gas		Inside wall	Outside wall	Cooling air	
	$T_{g,1/2}$	$T_{g,1/4}$	T_w	T_s	T_a	$T_{g,1/2}$	$T_{g,1/4}$	T_w	T_s	T_a	$T_{g,1/2}$	$T_{g,1/4}$	T_w	T_s	T_a	$T_{g,1/2}$	$T_{g,1/4}$	T_w	T_s	T_a	
CONFIGURATION B																					
1	1076	1039	602	72	74	1406	1073	743	123	152	2519	2202	1068	209	264	2758	2599	1254	377	373	1
2	1088	1026	549	60	65	1342	1064	688	99	133	2490	1923	986	161	221	2752	2598	1170	291	313	2
3	1076	1025	510	50	58	1306	1051	627	98	117	2424	2129	900	149	183	2706	2380	1089	221	270	3
4	1069	1031	477	51	56	1182	1082	592	89	109	2512	2009	856	143	169	2585	2404	1067	215	248	4
5	1077	1013	443	52	54	1332	1038	543	81	103	2459	1849	777	110	151	2727	2323	995	169	219	5
6	1083	1044	516	64	67	1382	1078	657	101	130	2500	1936	944	154	207	2718	2410	1164	286	296	6
7	1054	1041	628	290	293	1335	1066	726	321	338	2214	1788	972	361	388	2607	2232	1189	458	468	7
8	1061	1052	635	296	300	1403	1088	737	326	345	2488	1729	989	364	395	2680	2488	1196	463	473	8
9	1073	1067	691	382	389	1427	1111	794	411	431	2307	1797	1052	451	479	2746	2543	1251	543	557	9
10	1099	1031	744	476	485	1437	1128	842	499	521	2415	1977	1077	548	564	2703	2552	1284	635	637	10
11	1068	1060	797	569	583	1402	1118	886	583	583	2491	1932	1106	635	641	2452	2194	1278	692	701	11
12	1070	1073	851	659	671	1412	1124	939	670	696	2245	1958	1156	726	726	2723	2344	1333	780	784	12
13	1089	1100	914	753	768	1452	1153	1008	761	788	2300	2037	1221	804	814	2509	2325	1379	898	869	13
CONFIGURATION C																					
1	1101	1073	575	92	78	1241	1107	654	140	146	1610	1190	800	179	201	1987	1639	928	259	267	1
2	1102	1074	668	271	271	1254	1101	725	304	322	1646	1323	856	345	359	2015	1647	945	440	413	2
3	1112	1087	727	367	377	1258	1117	780	390	421	1603	1322	911	433	449	1994	1639	999	513	498	3
4	1115	1093	780	463	473	1255	1122	831	483	511	1625	1332	958	526	537	2000	1647	1045	596	582	4
5	1117	1095	845	572	585	1258	1128	892	585	627	1624	1321	1014	625	636	1990	1649	1096	683	675	5
6	1135	1115	963	764	778	1278	1152	1009	768	802	1560	1364	1126	796	813	2020	1701	1209	850	843	6
7	1142	1127	1091	971	991	1283	1167	1134	967	1003	1682	1374	1241	994	1003	2029	1718	1310	1027	1026	7
8	1069	1069	501	64	65	1402	1088	567	96	119	2121	1670	805	130	168	2512	2200	993	224	233	8

[redacted]

[redacted]

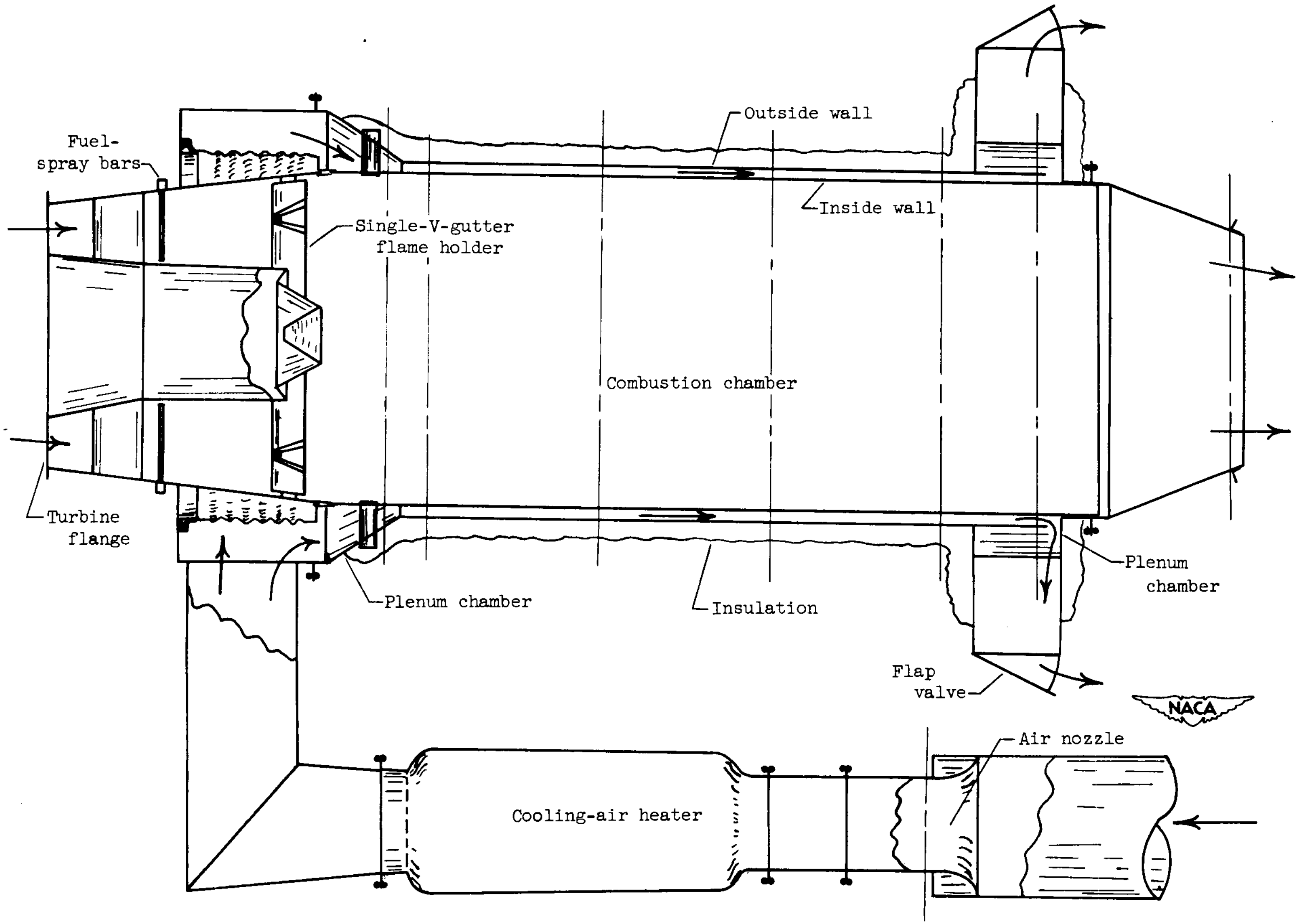

Figure 1. - Tail-pipe burner assembly.

[redacted]

2408

2408

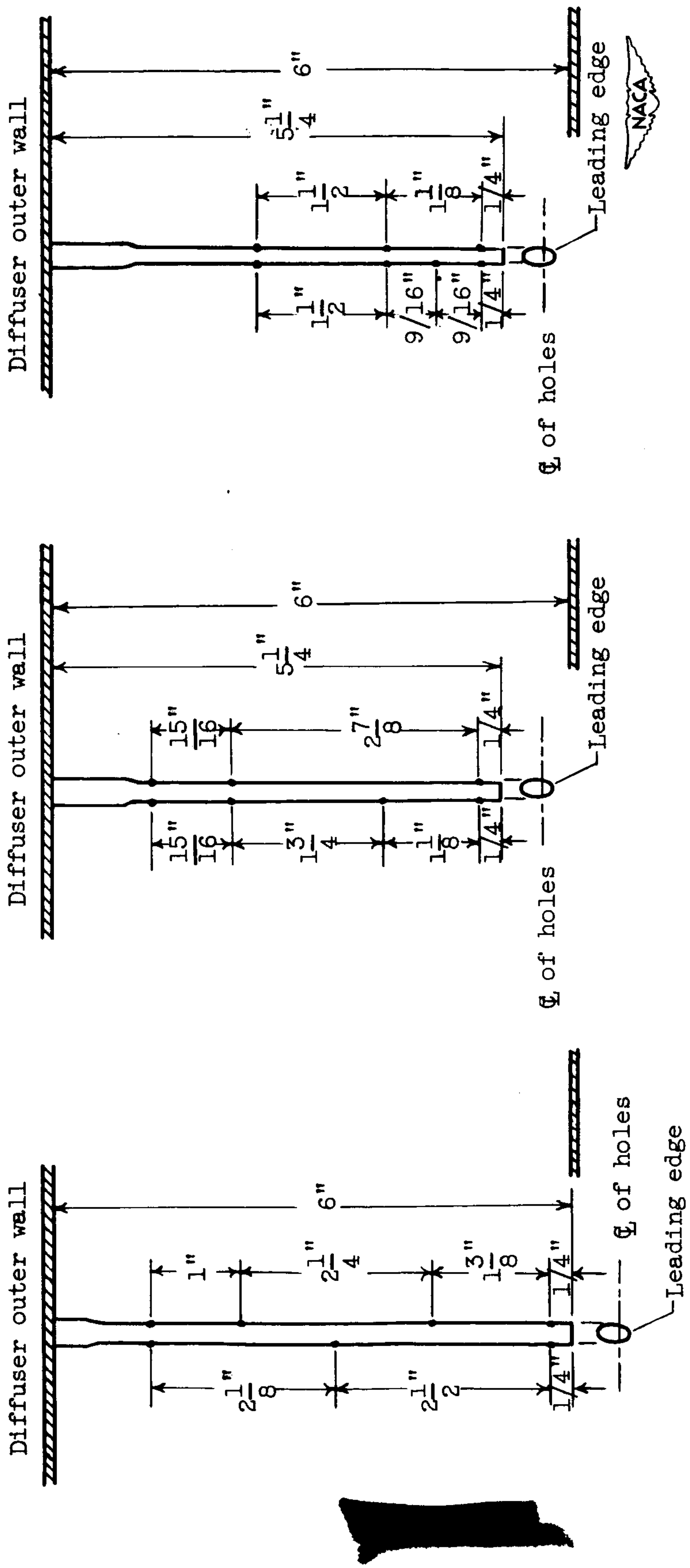

(a) Nearly uniform fuel distribution.

(b) Fuel distribution concentrated toward outside of burner.

(c) Fuel distribution concentrated toward center of burner.

Figure 2. - Fuel-spray bars.

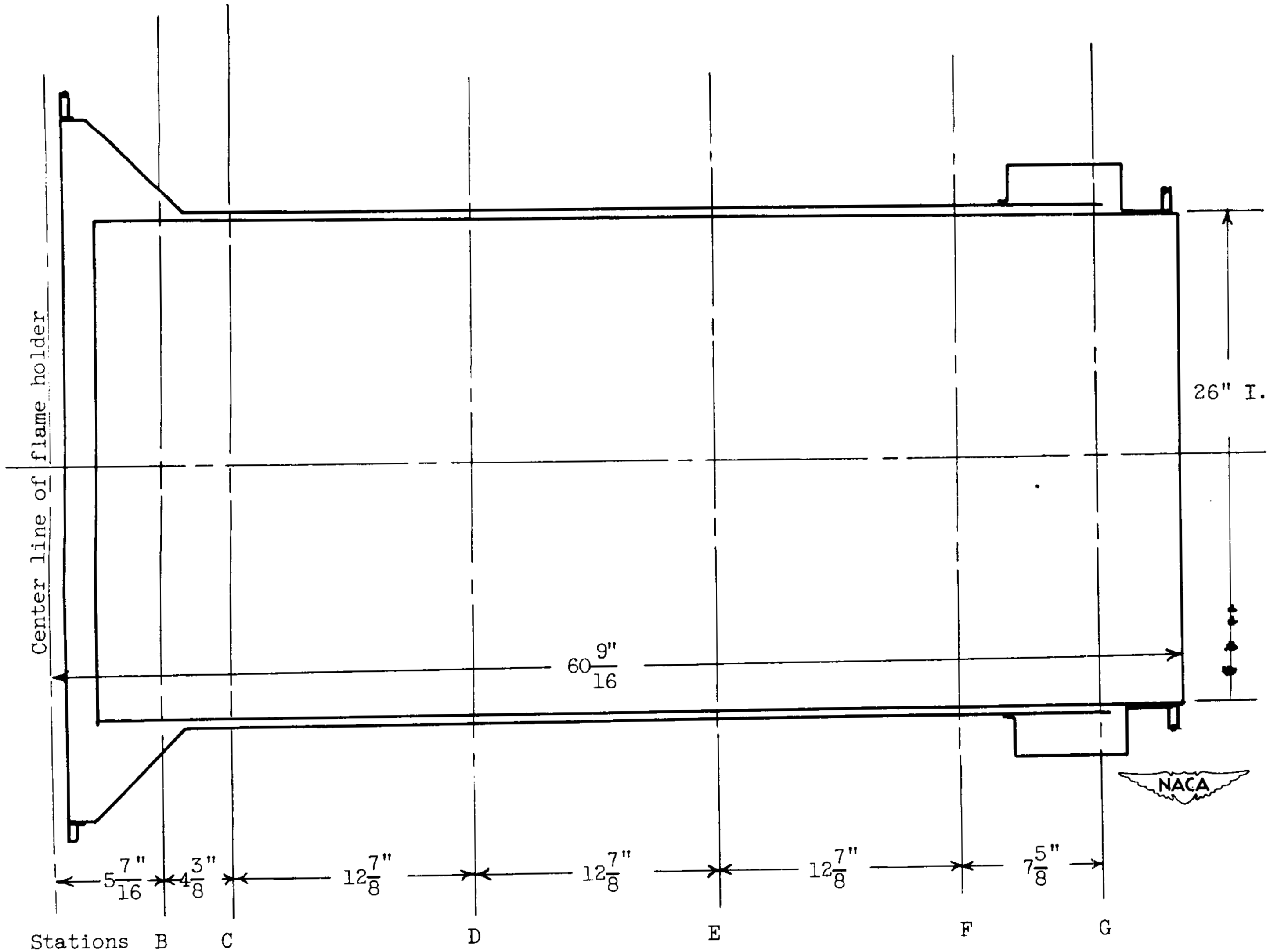

Figure 3. - Instrumentation stations on the tail-pipe burner.

2408

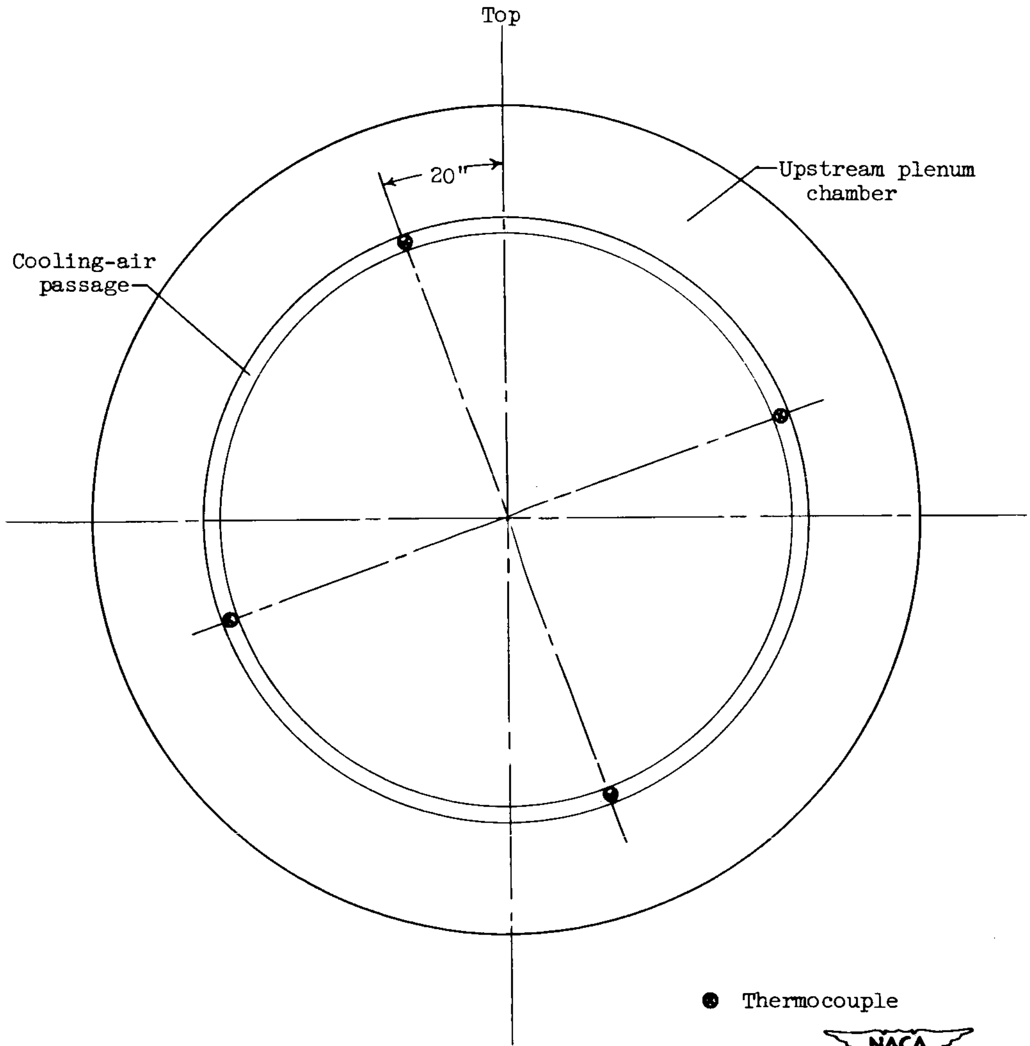

(a) Station B, cooling-passage inlet, looking downstream.

Figure 4. - Location of instrumentation.

2408

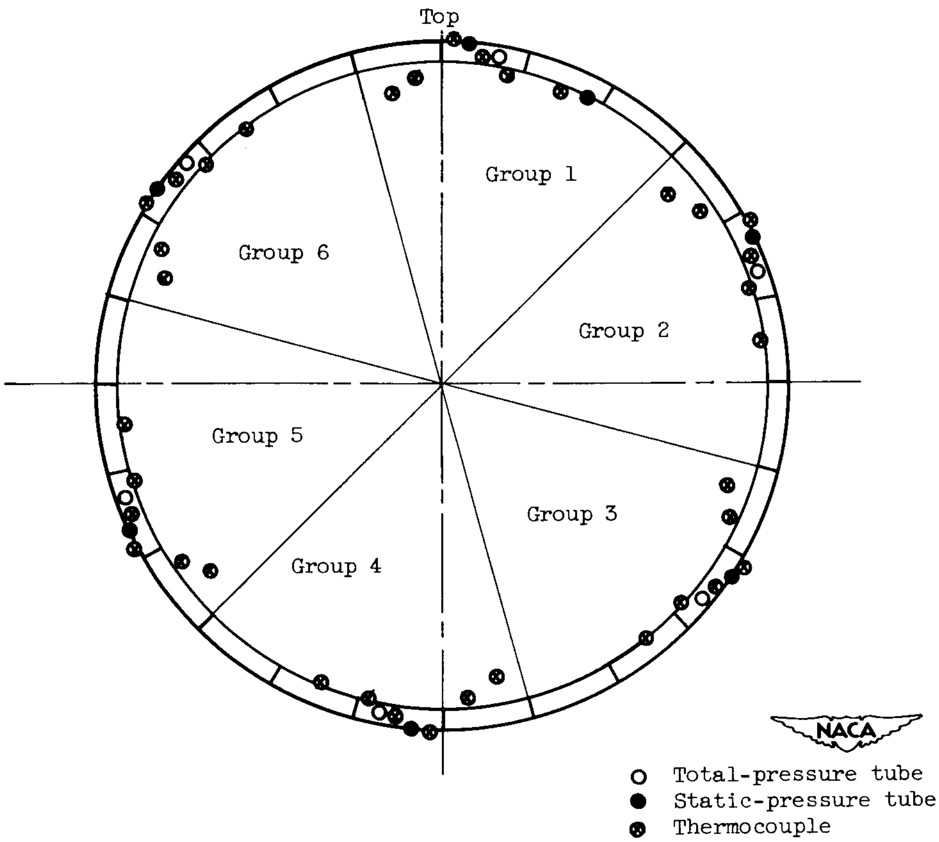

(b) Stations C through E, looking downstream.

Figure 4. - Continued. Location of instrumentation.

[redacted]

2408

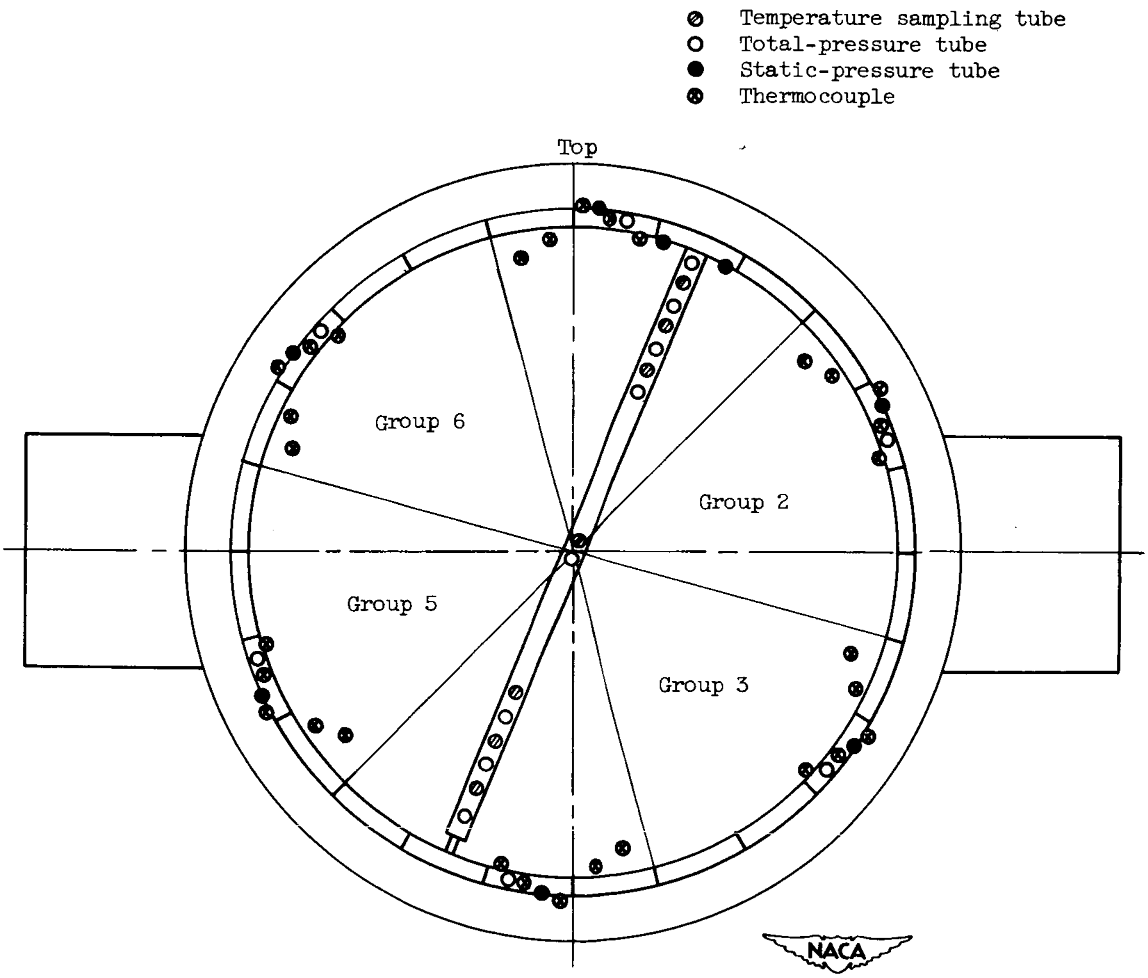

(c) Station F, looking downstream.

Figure 4. - Continued. Location of instrumentation.

[redacted]

2408

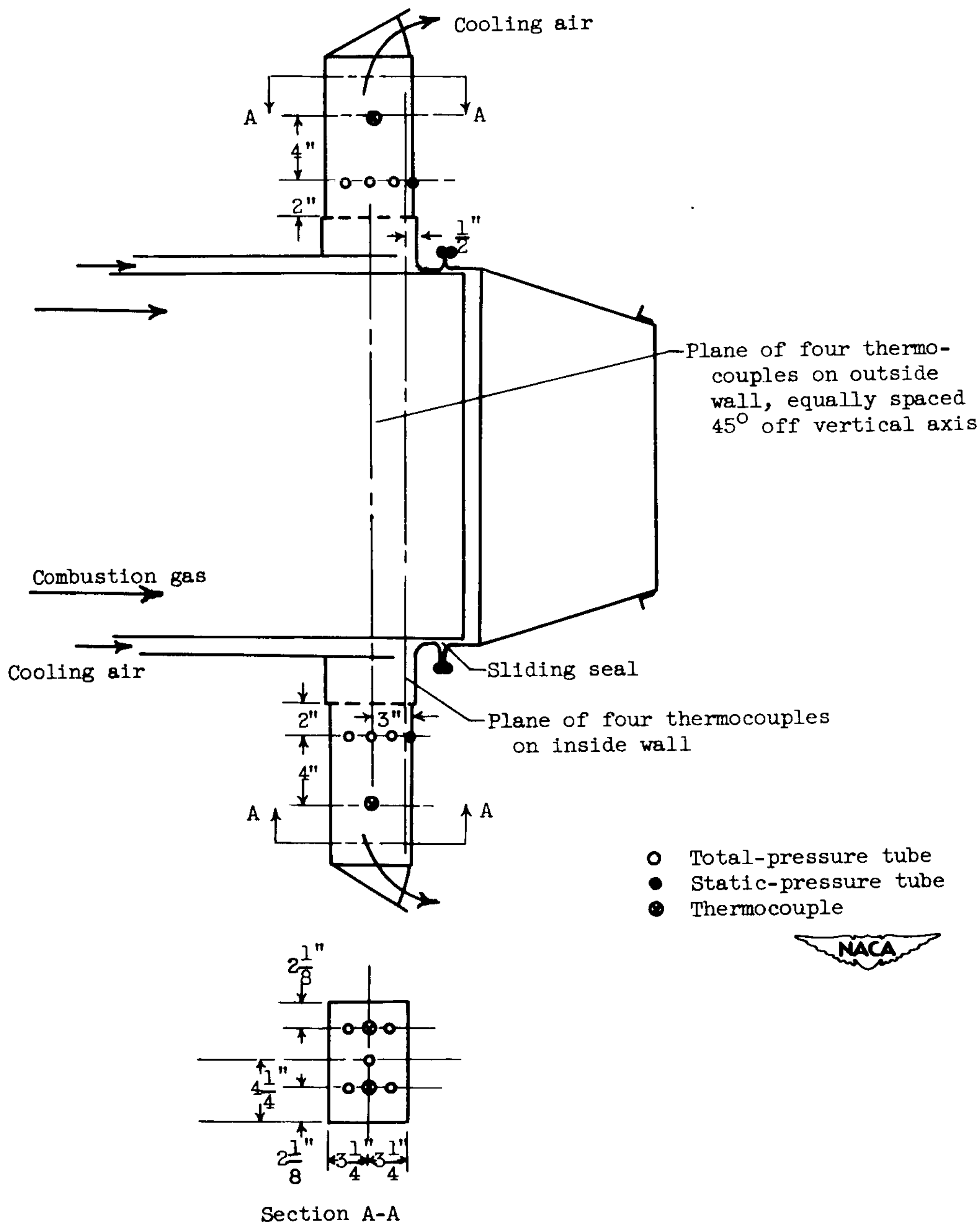

(d) Station G.

Figure 4. - Continued. Location of instrumentation.

[redacted]

2408

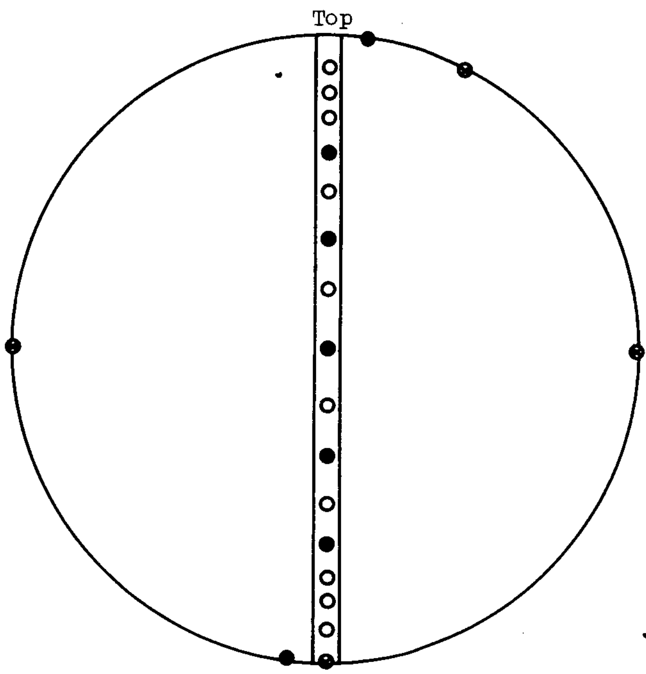

- Thermocouple
- Total-pressure tube
- Static-pressure tube

(e) Exhaust-nozzle exit, looking downstream.

Figure 4. - Continued. Location of instrumentation.

2408

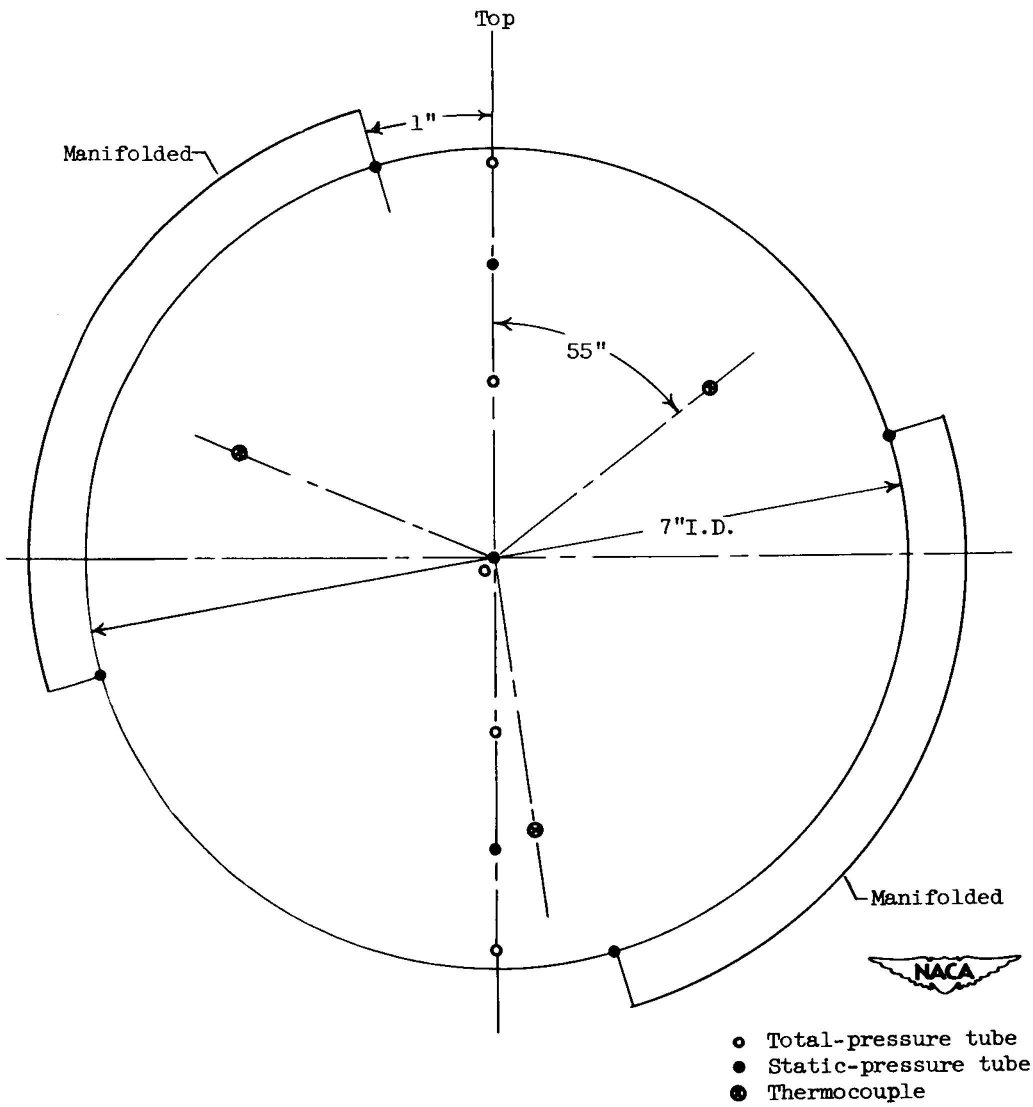

(f) Throat of cooling-air metering nozzle.

Figure 4. - Continued. Location of instrumentation.

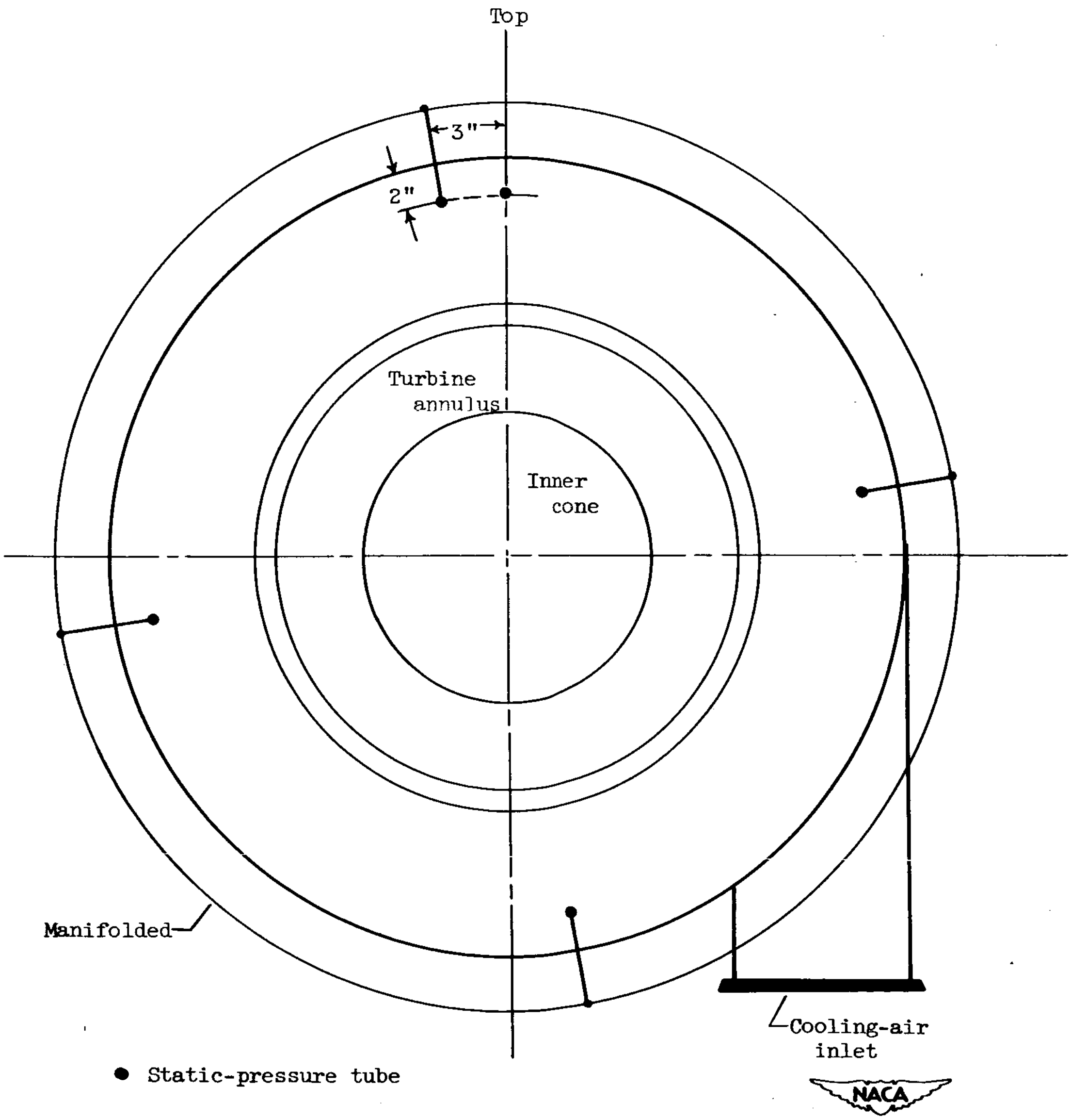

(g) Cooling-air inlet plenum chamber, looking downstream.

Figure 4. - Concluded. Location of instrumentation.

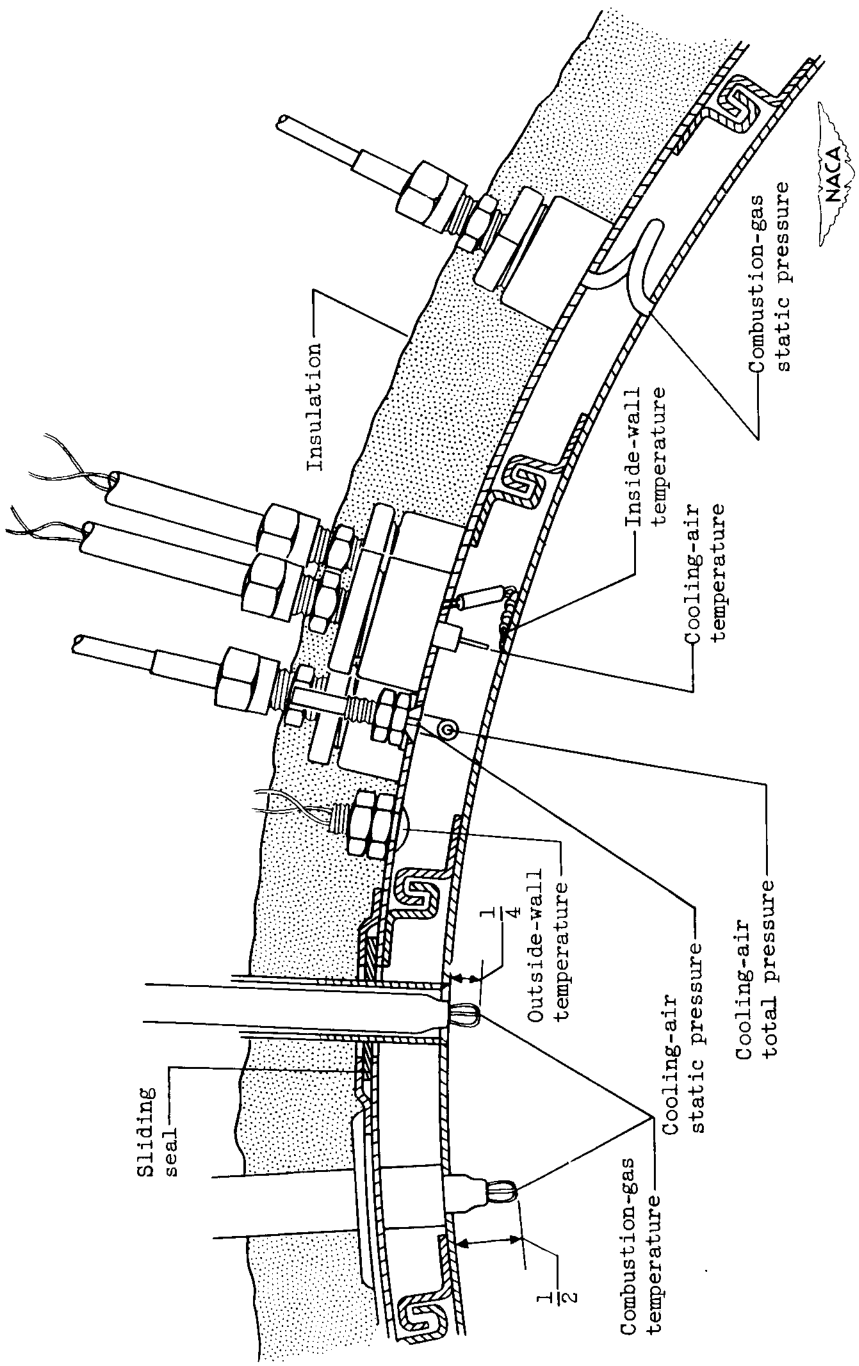

Figure 5. - Typical instrumentation group for stations C to F.

2408

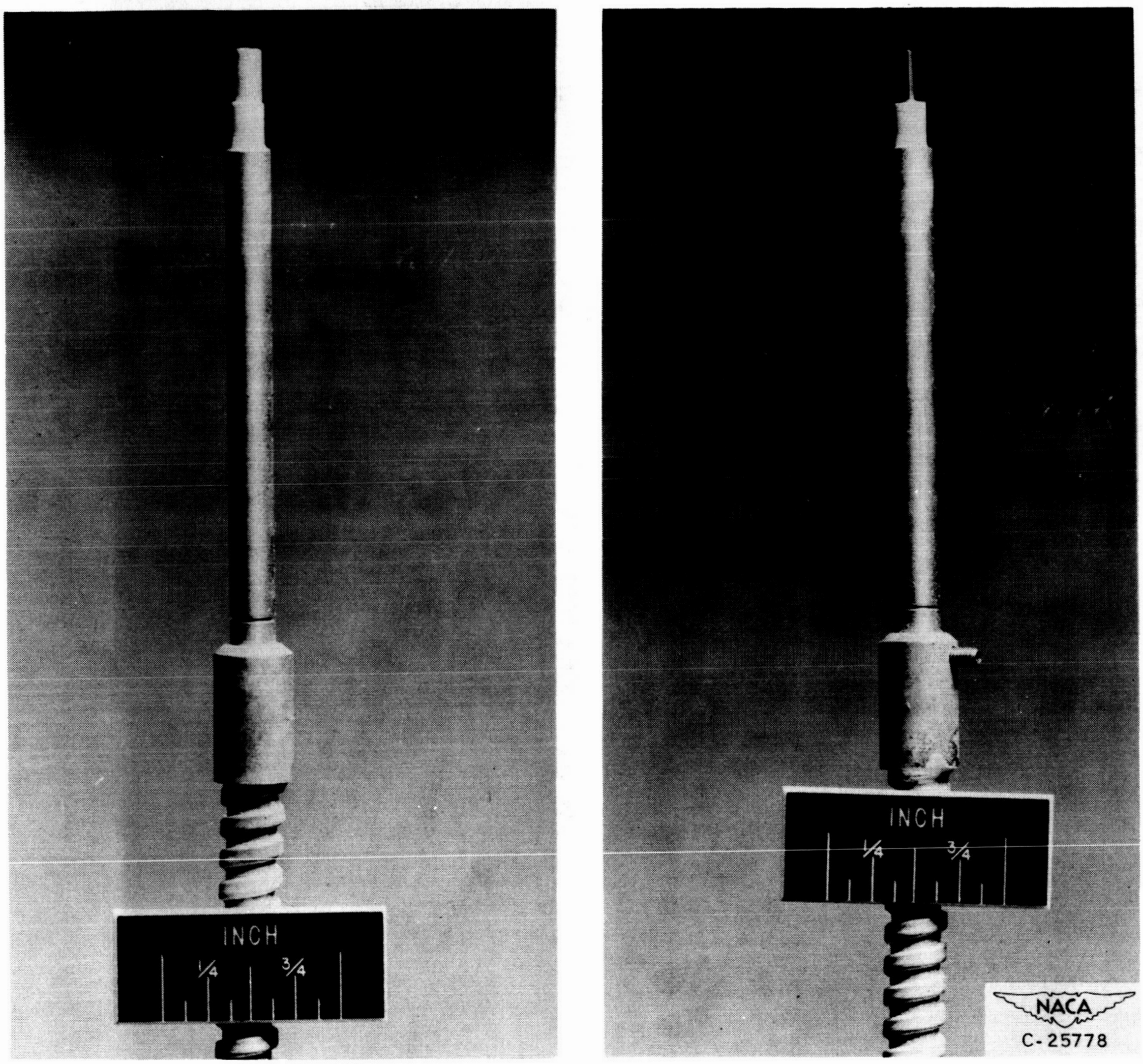

Figure 6. - National Bureau of Standards type shielded thermocouple for cooling-air temperature measurement.

[redacted]

2408

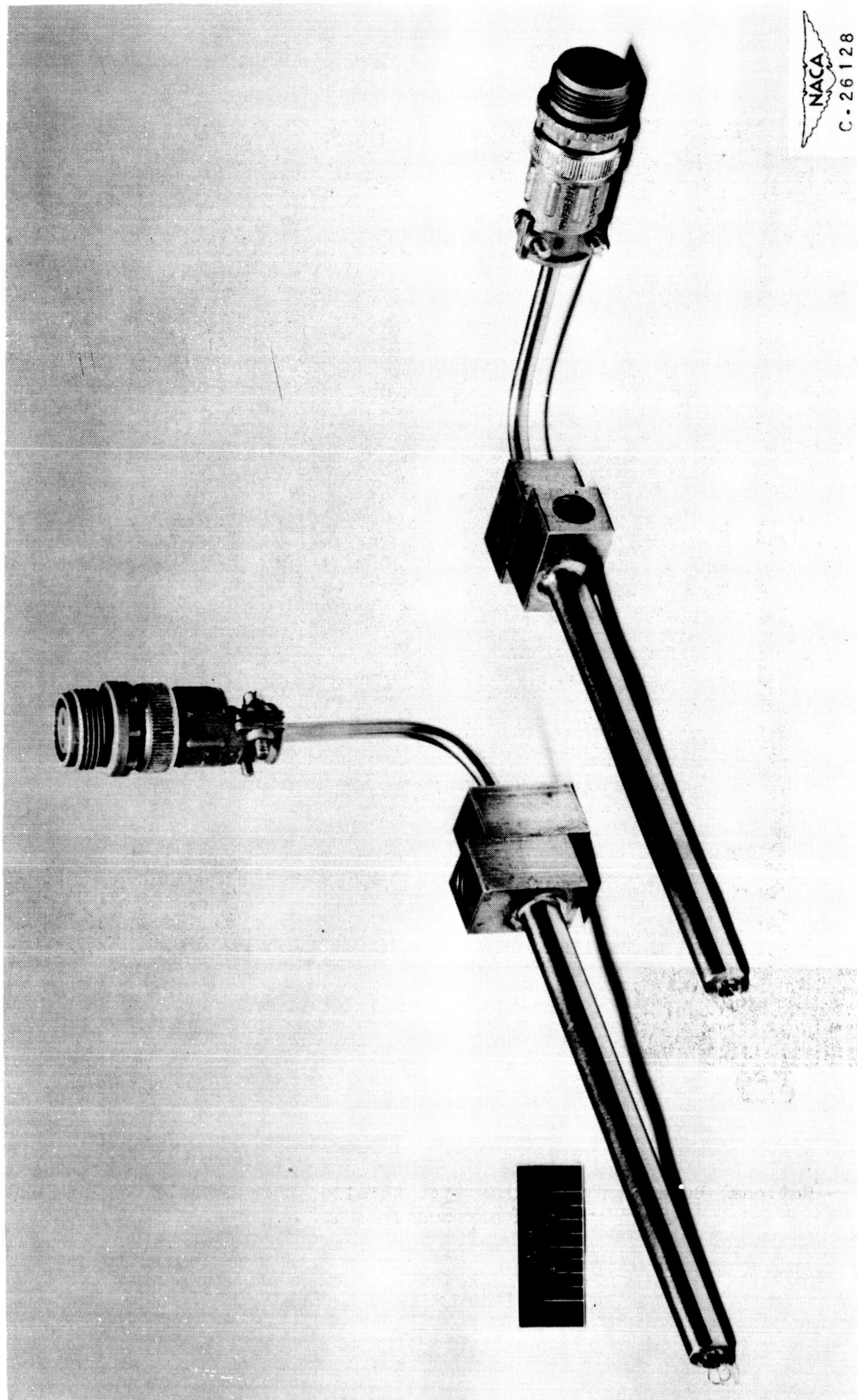

Figure 7. - Platinum-rhodium - platinum thermocouple probes.

[redacted]

2408

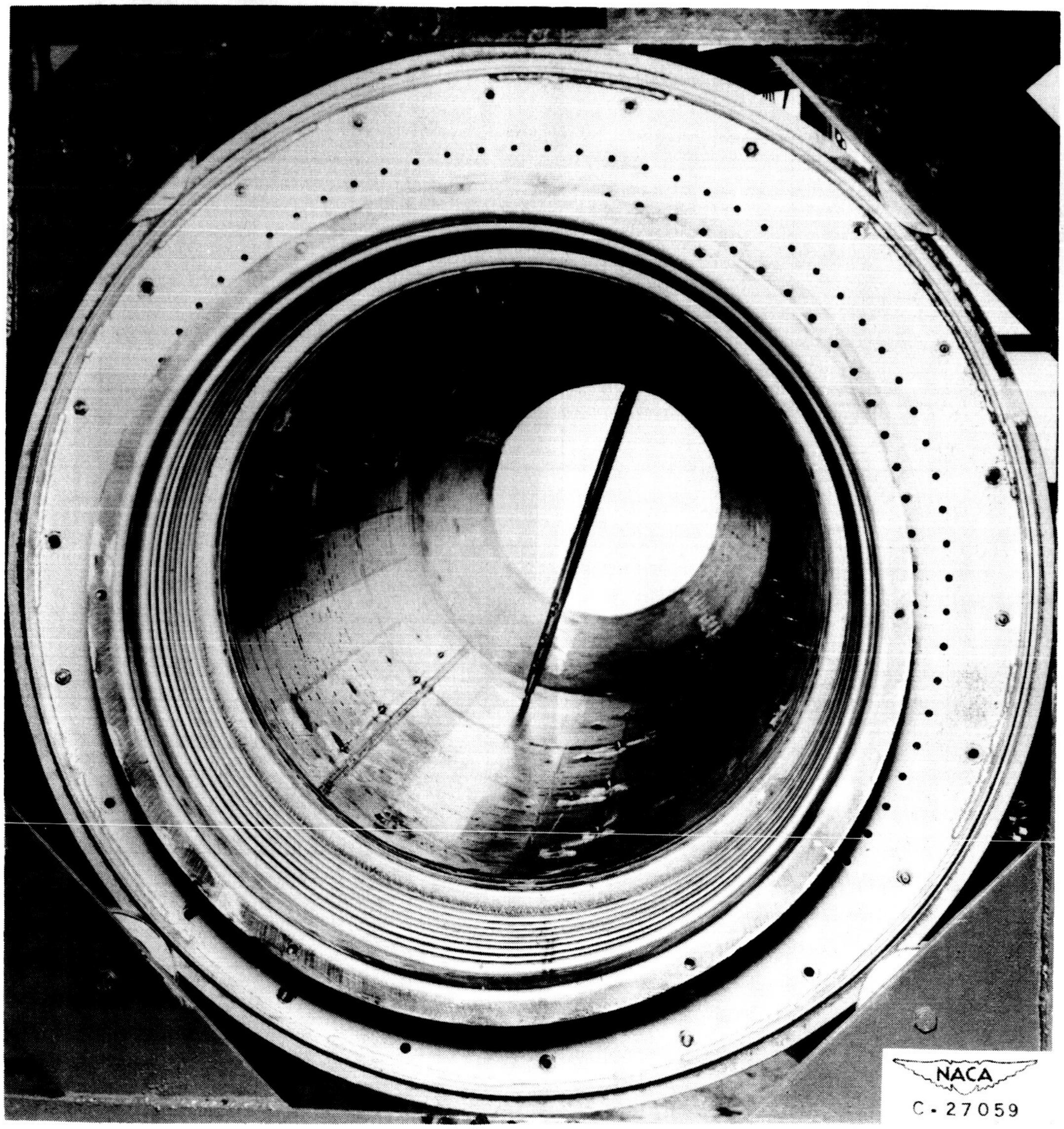

Figure 8. - Interior view of combustion chamber showing installation of sonic-flow orifice rake and platinum-rhodium - platinum thermocouples.

[redacted]

2408

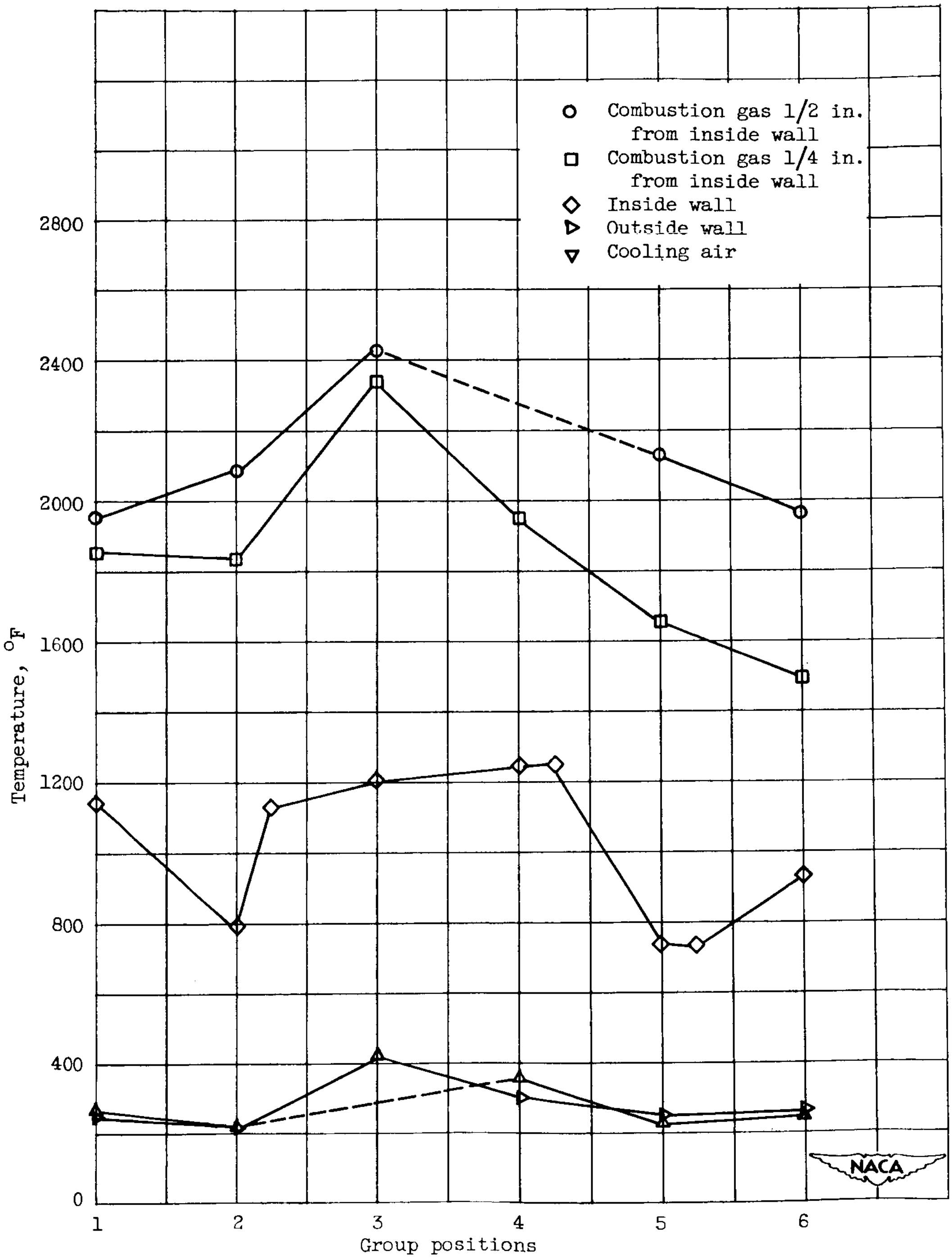

(a) Accumulated afterburner time, 32 minutes; exhaust-gas total temperature, 2993° R; mass-flow ratio, 0.1006; inlet cooling-air temperature, 526° R.

Figure 9. - Circumferential temperature variations at station F, configuration A.

[redacted]

2408

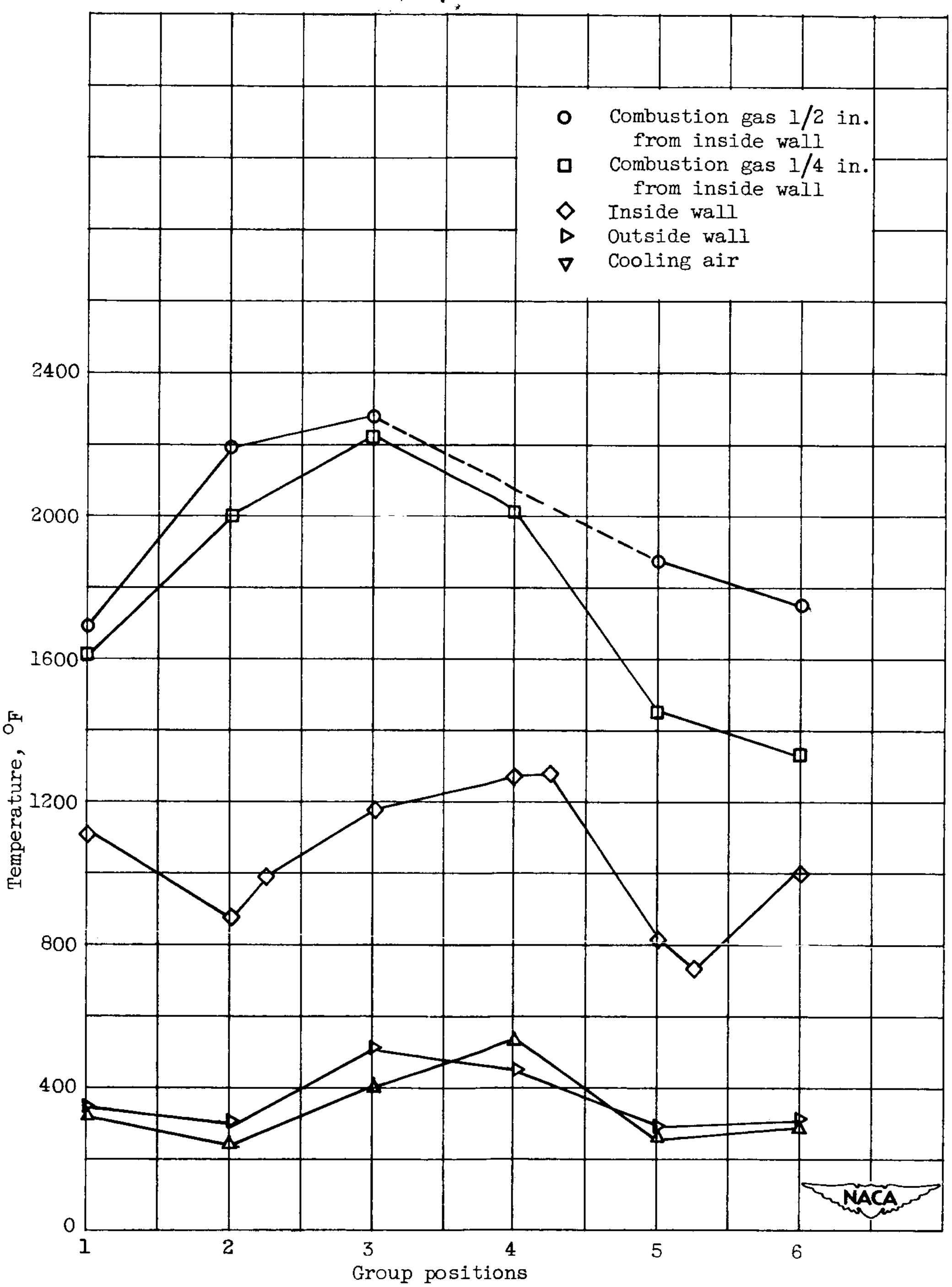

(b) Accumulated afterburner time, 3 hours and 36 minutes; exhaust-gas total temperature approximately 3060° R; mass-flow ratio, 0.0949; inlet cooling-air temperature, 536° R.

Figure 9. - Continued. Circumferential temperature variations at station F, configuration A.

[redacted]

2408

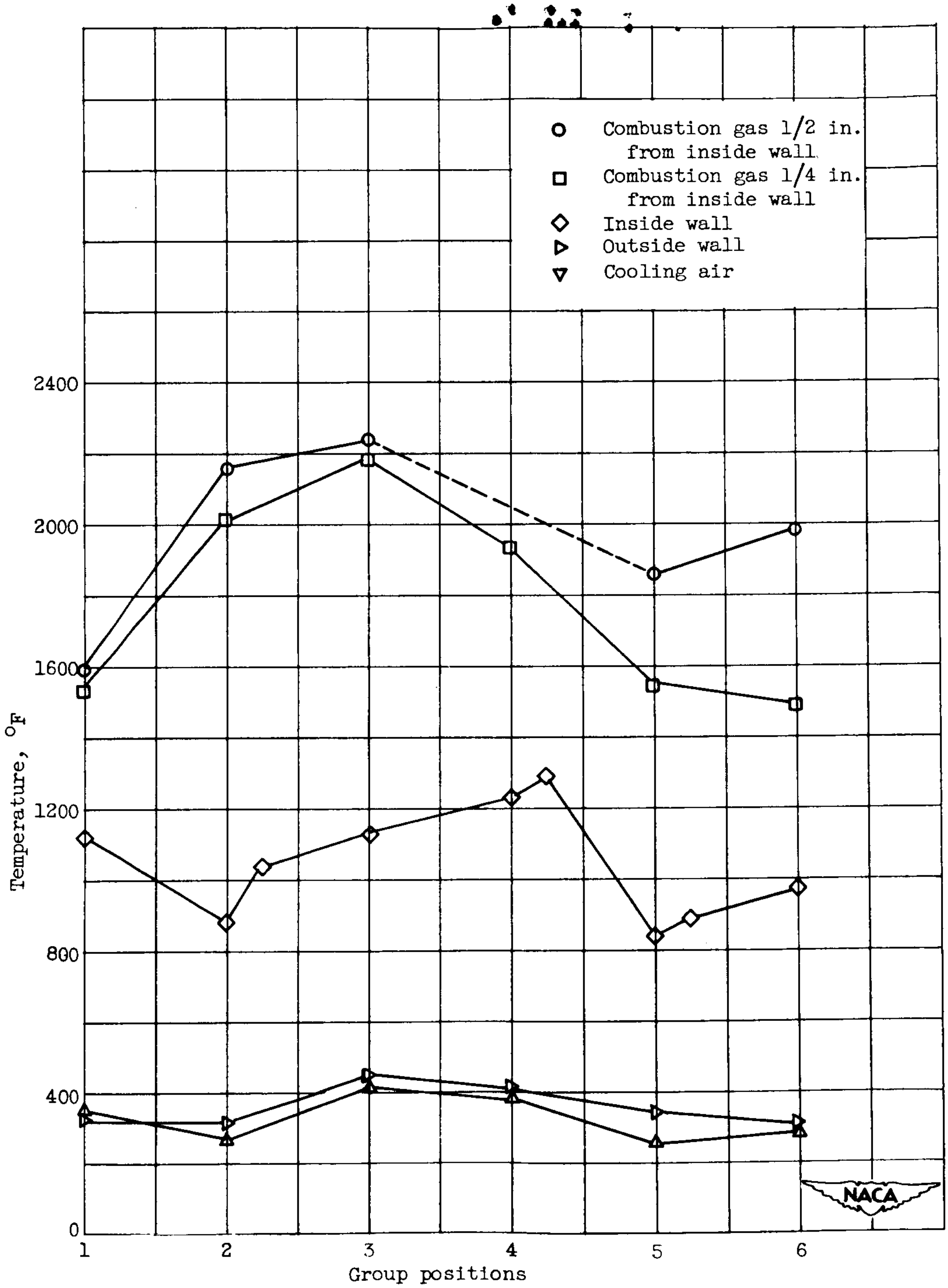

(c) Accumulated afterburner time, 9 hours and 22 minutes; exhaust-gas total temperature, 3102° R; mass-flow ratio, 0.0985; inlet cooling-air temperature, 529° R.

Figure 9. - Continued. Circumferential temperature variations at station F, configuration A.

[redacted]

2408

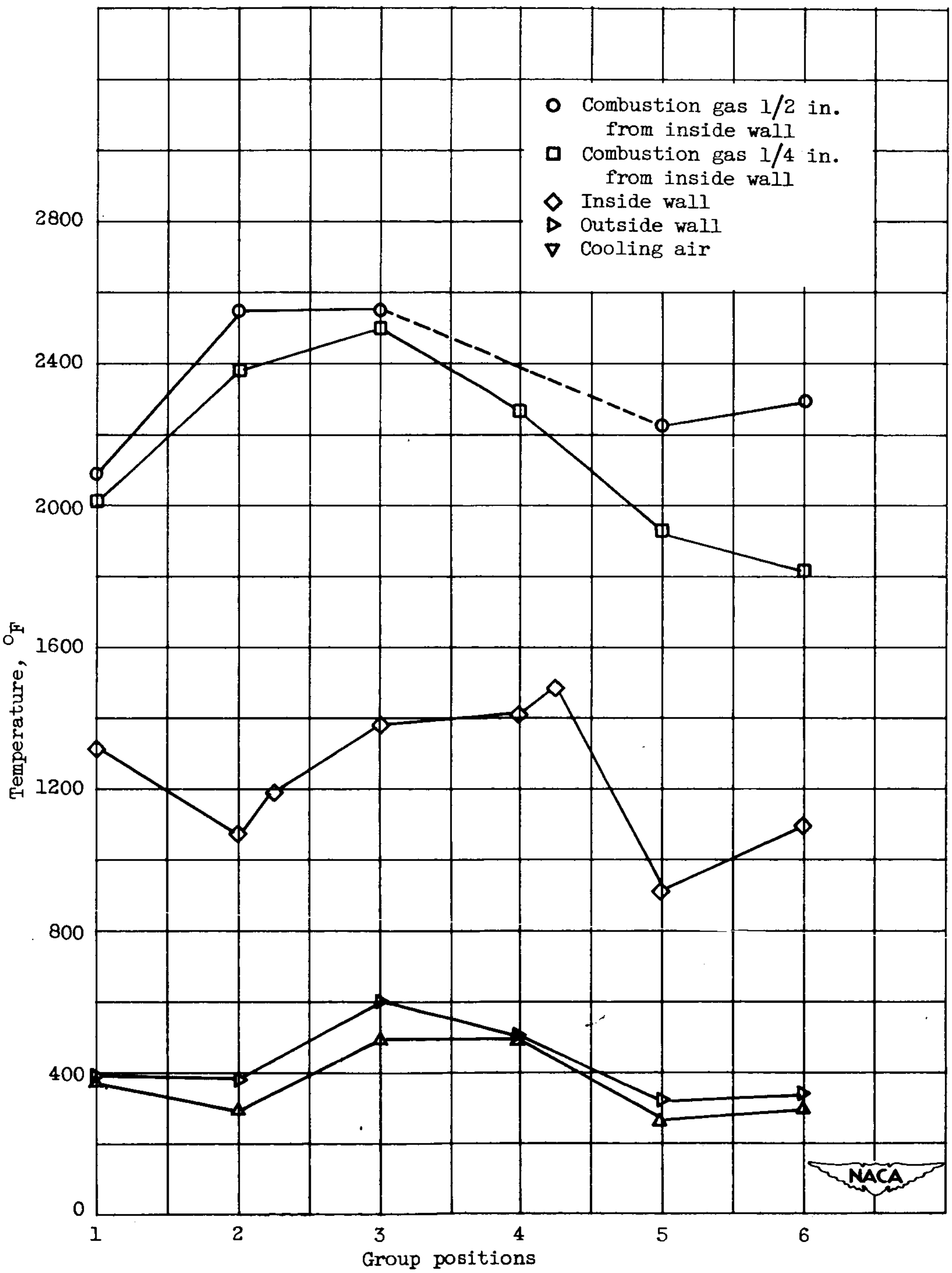

(d) Accumulated afterburner time, 3 hours and 48 minutes; exhaust-gas total temperature, 3484° R; mass-flow ratio, 0.1050; inlet cooling-air temperature, 530° R.

Figure 9. - Concluded. Circumferential temperature variations at station F, configuration A.

[redacted]

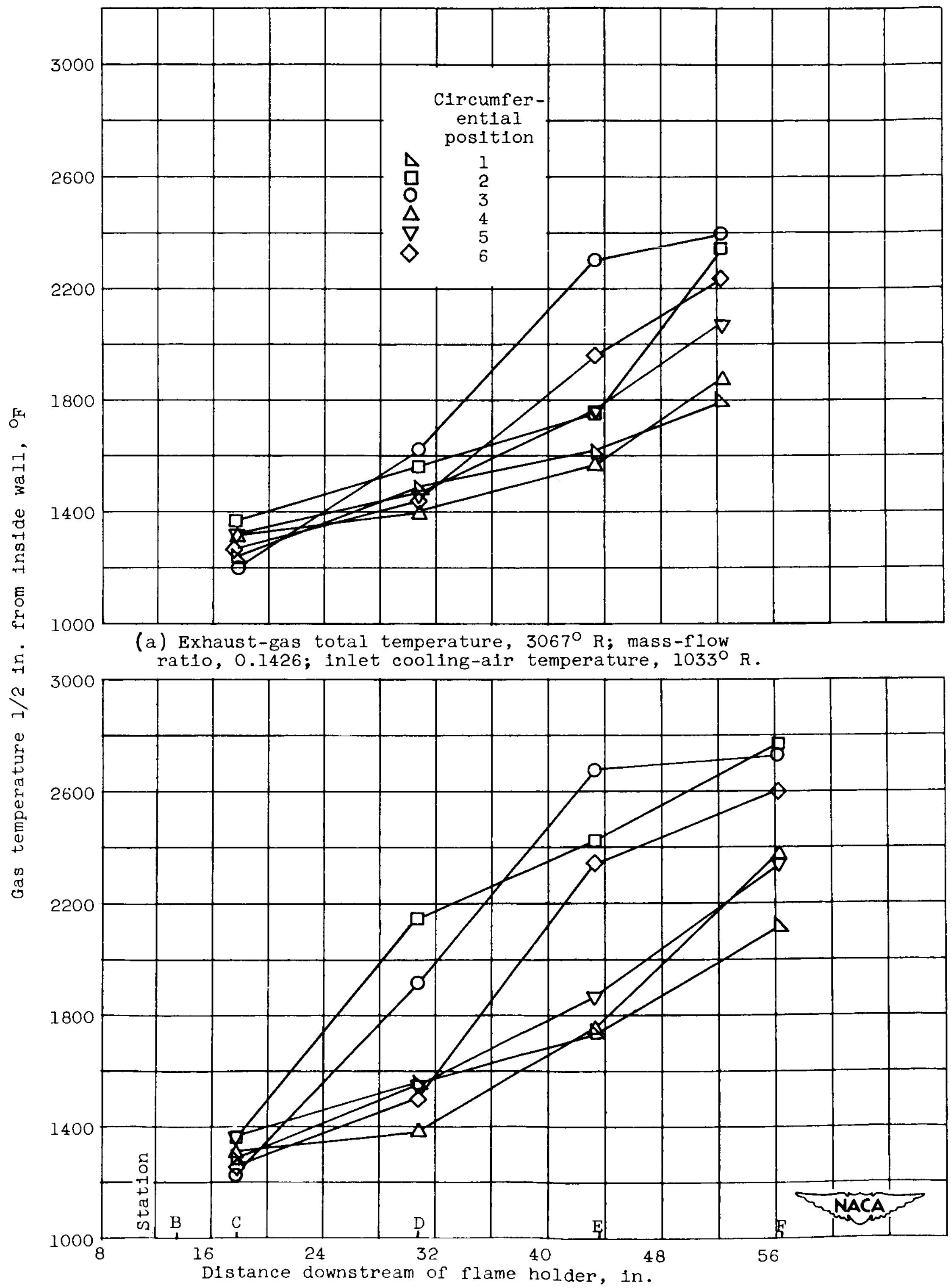

(a) Exhaust-gas total temperature, 3067° R; mass-flow ratio, 0.1426; inlet cooling-air temperature, 1033° R.

(b) Exhaust-gas total temperature, 3394° R; mass-flow ratio, 0.1436; inlet cooling-air temperature, 539° R.

Figure 10. - Longitudinal gas-temperature profiles 1/2 inch from inside wall, configuration A.

[redacted]

2408

2408

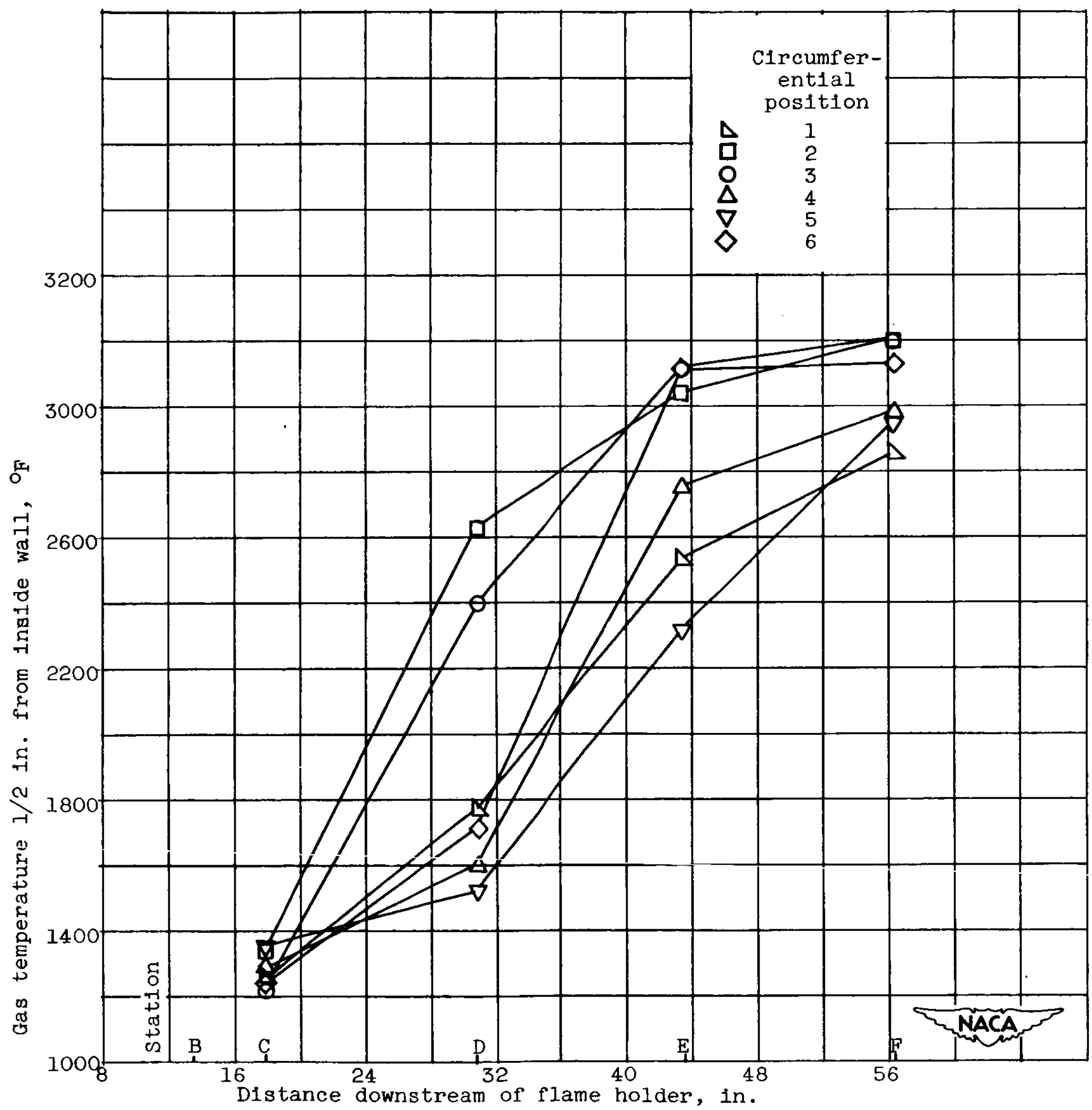

(c) Exhaust-gas total temperature, 3811° R; mass-flow ratio, 0.1374; inlet cooling-air temperature, 538° R.

Figure 10. - Concluded. Longitudinal gas-temperature profiles 1/2 inch from inside wall, configuration A.

[redacted]

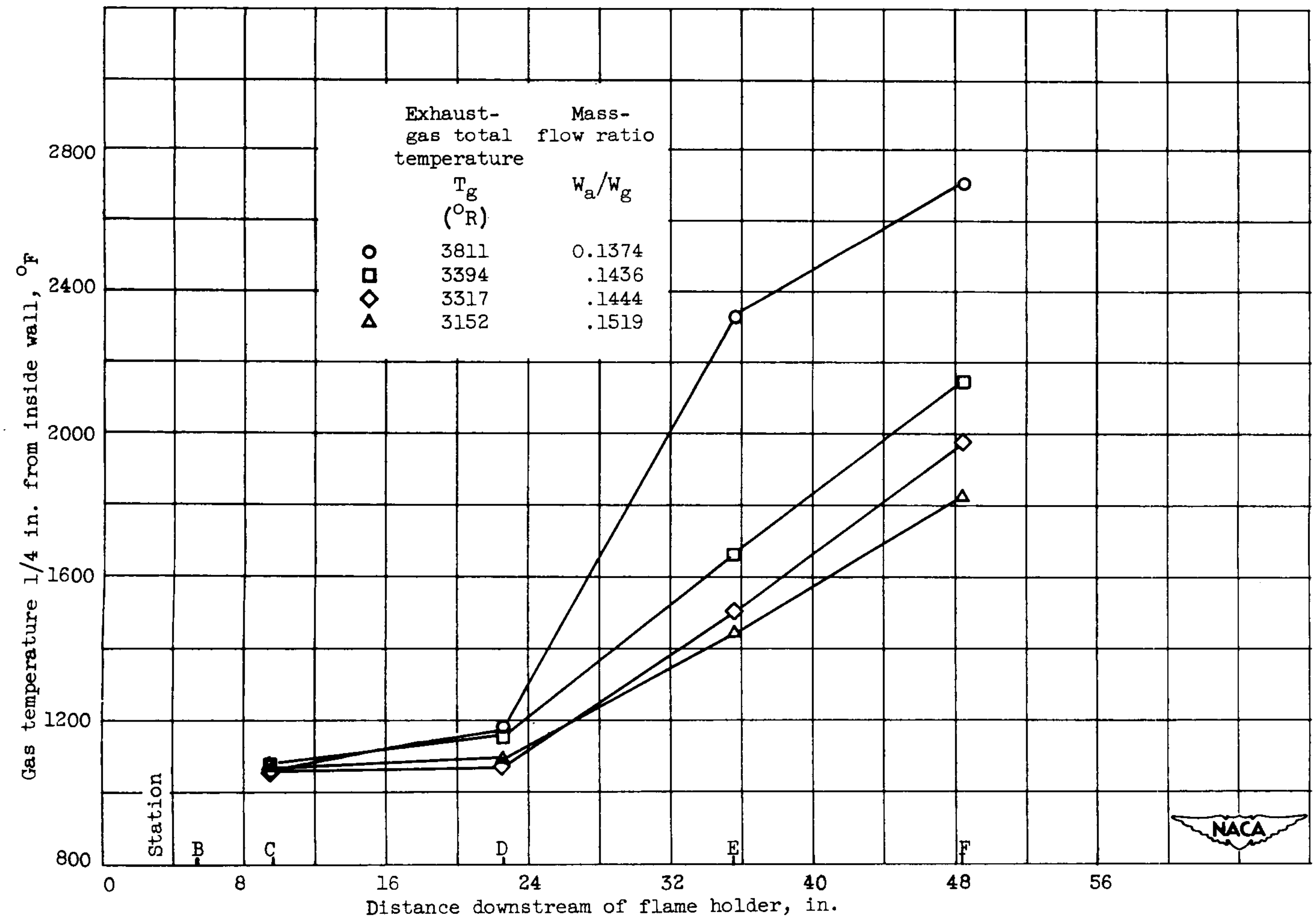

(a) Temperature 1/4 inch from inside wall.

Figure 11. - Variation of longitudinal profile of exhaust-gas temperature near inside wall with exhaust-gas temperature for configuration A. Approximate inlet cooling-air temperature, 520° R.

2408

[redacted]

2408

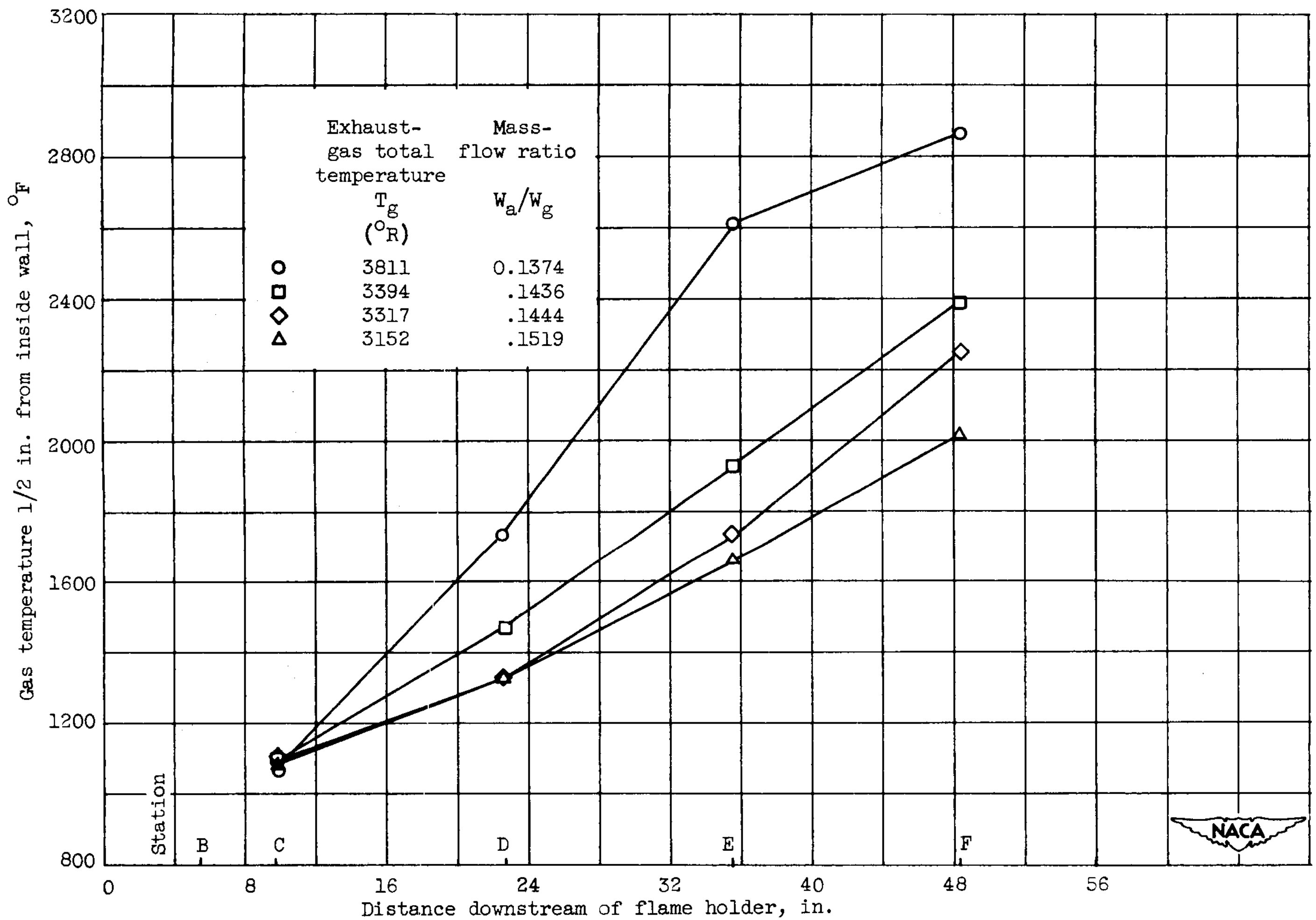

(b) Temperature 1/2 inch from inside wall.

Figure 11. - Concluded. Variation of longitudinal profile of exhaust-gas temperature near inside wall with exhaust-gas temperature for configuration A. Approximate inlet cooling-air temperature, 520° R.

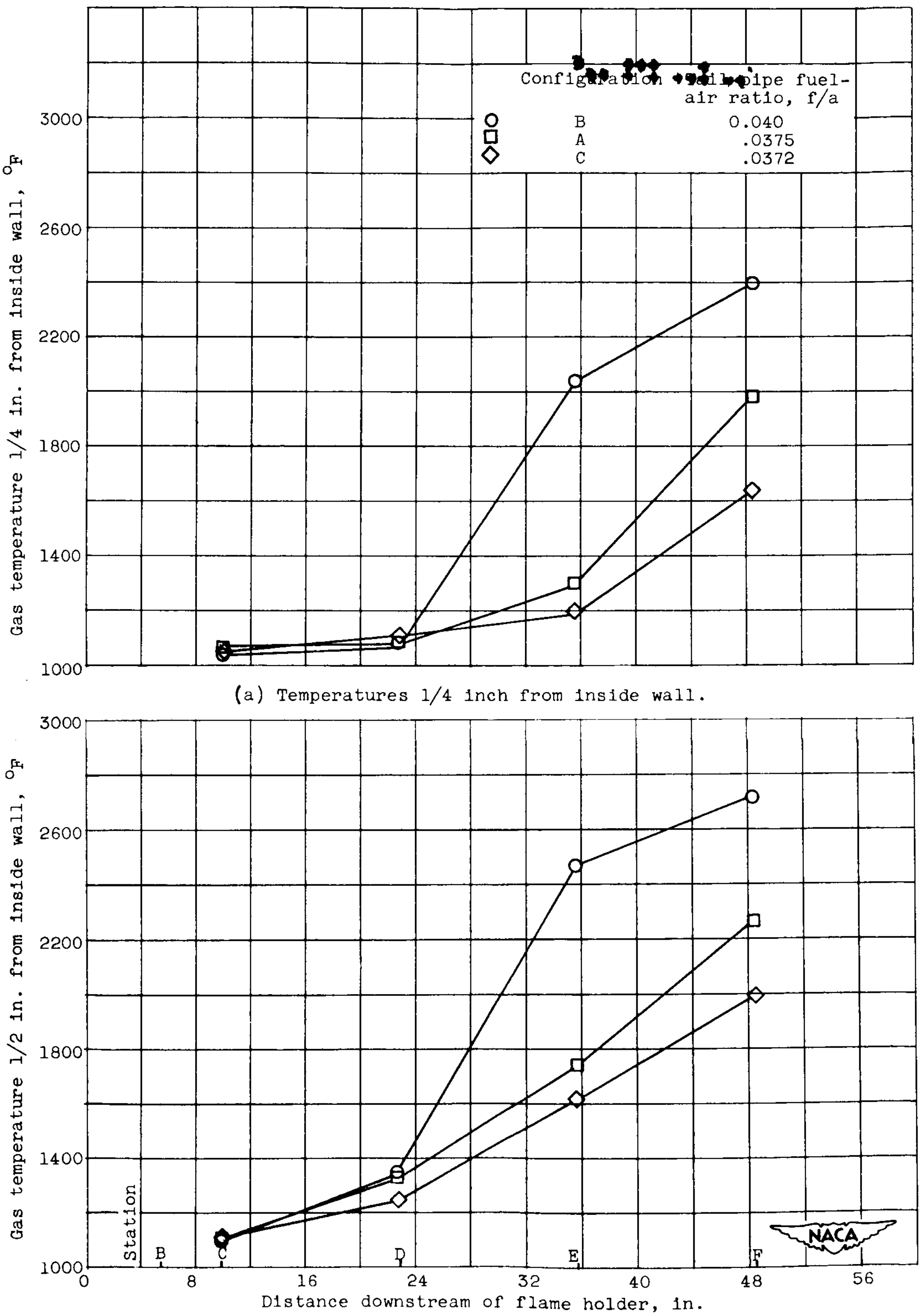

(a) Temperatures 1/4 inch from inside wall.

(b) Temperatures 1/2 inch from inside wall.

Figure 12. - Effect of fuel distribution on gas temperatures near inside wall. Exhaust-gas total temperature, approximately 3230° R; mass-flow ratio, 0.145; cooling-air inlet temperature, 510° R.

[redacted]

2408

2408

	Exhaust-gas total temperature	Mass-flow ratio	Inlet cooling-air temperature	Tail-pipe fuel-air ratio	Combustion-gas flow	Turbine-outlet total pressure	Turbine-discharge temperature
	T_g (^{o}R)	W_a/W_g	$T_{a,B}$ (^{o}R)	f/a	W_g (lb/sec)	(lb/sq ft abs.)	(^{o}R)
○	3394	0.1436	520	0.0441	22.29	1401	1626
□	3284	.1451	528	.0365	13.85	859	1620

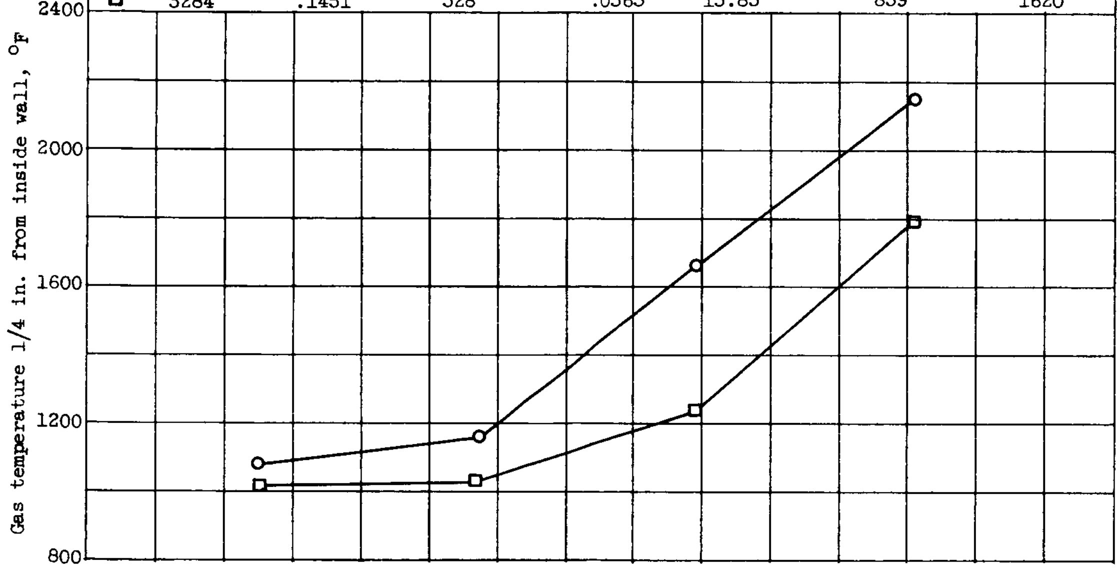

(a) Temperatures 1/4 inch from inside wall.

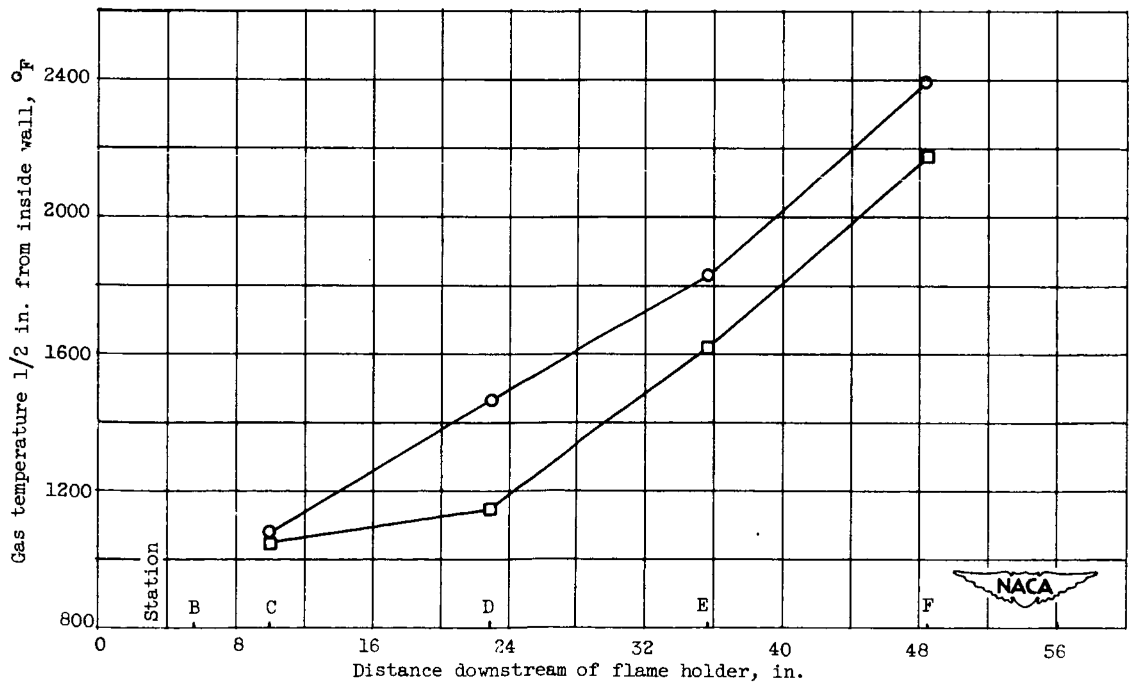

(b) Temperatures 1/2 inch from inside wall.

Figure 13. - Effect of combustion-gas mass flow on gas temperatures near inside wall for configuration A.

[redacted]

2408

	Exhaust-gas total temperature T_g (°R)	Mass-flow ratio W_a/W_g	Inlet cooling-air temperature $T_{a,B}$ (°R)	Tail-pipe fuel-air ratio f/a	Average inside-wall temperature T_w (°F)	Combustion-gas flow W_g (lb/sec)	Turbine-outlet total pressure (lb/sq ft abs.)
○	2994	0.0672	541	0.0325	1198	21.89	1373
□	2858	.0814	530	.0315	1107	21.98	1350
◇	3306	.1418	1340	.0363	1298	13.61	847
△	3272	.1415	548	.0385	1065	13.78	853
▽	3425	.1411	771	.0450	1158	22.04	1394
◺	3403	.1412	1408	.0444	1401	22.38	1409

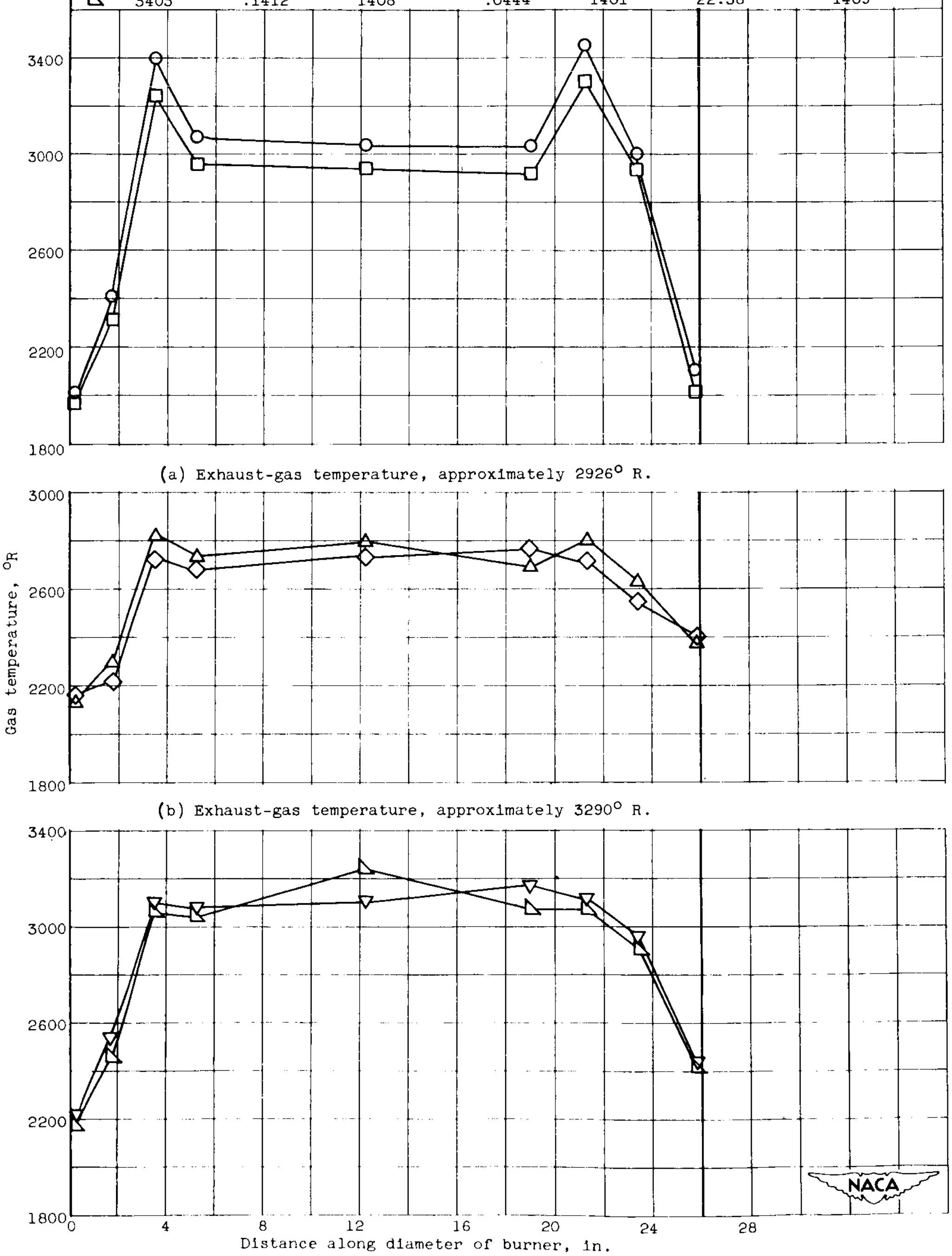

(a) Exhaust-gas temperature, approximately 2926° R.

(b) Exhaust-gas temperature, approximately 3290° R.

(c) Exhaust-gas temperature, approximately 3414° R.

Figure 14. - Transverse profiles of combustion-gas temperature at station F, configuration A.

[redacted]

2408

Symbol	Exhaust-gas total temperature T_g (°R)	Mass-flow ratio W_a/W_g	Inlet cooling air temperature $T_{a,B}$ (°R)	Tail-pipe fuel-air ratio f/a	Average inside-wall temperature T_w (°F)	Combustion-gas flow W_g (lb/sec)	Turbine-outlet total pressure (lb/sq ft abs.)	Average gas temperature 1/4 in. from inside wall $T_{g,1/4}$ (°R)
○		0.1430	534	0.0393		22.37		2448
□	3266	.1917	513	.0391	866	22.01		2354
◇	3305	.1449	495	.0409	1164	22.02	1416	2870
△	3215	.1422	500	.0399	1089	22.23	1410	2840
▽	3214	.1426	828	.0371	999	22.37	1415	2099
◺	3251	.1389	1040	.0370	1096	22.32	1419	2109

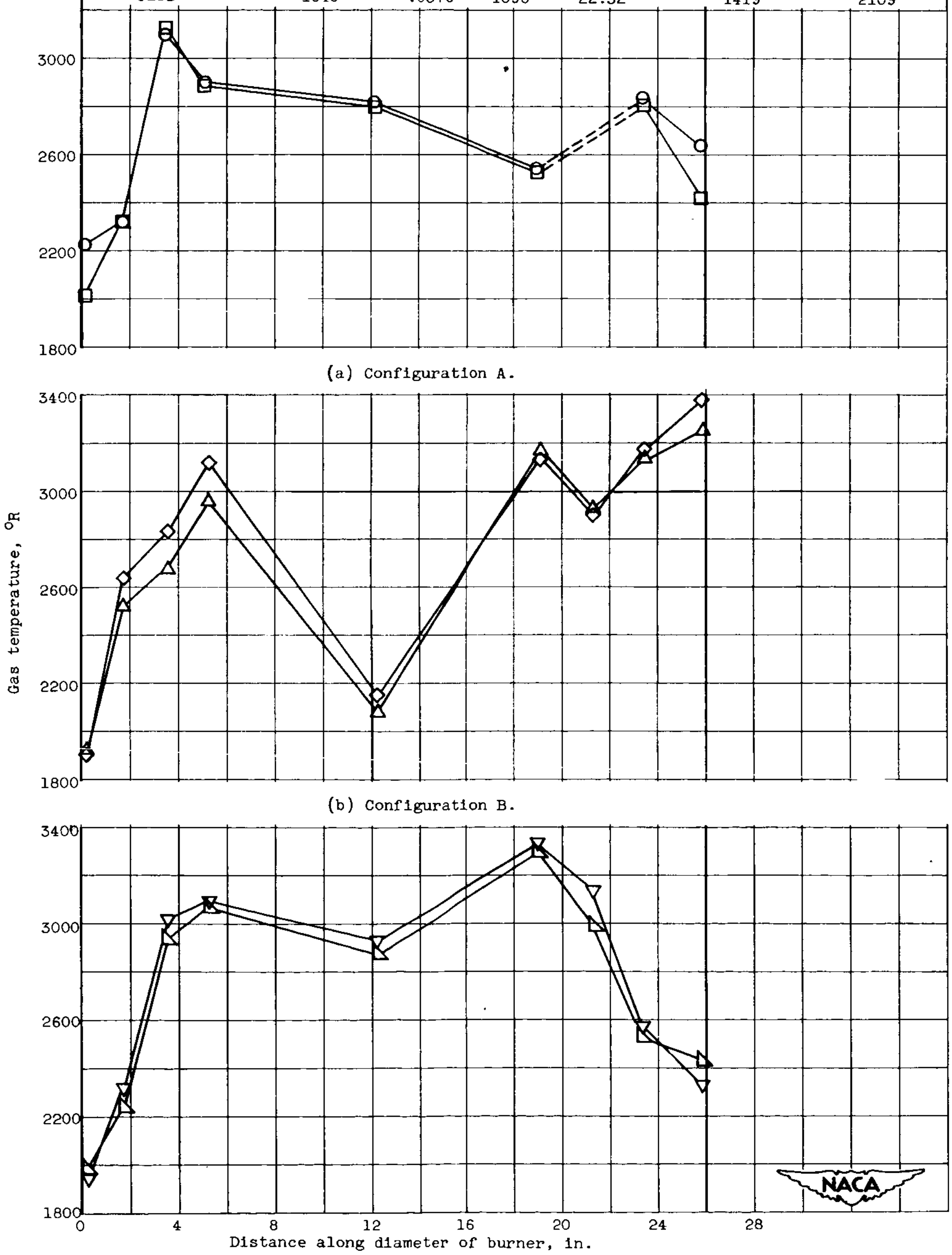

(c) Configuration C.

Figure 15. - Effect of fuel distribution on transverse profiles of combustion-gas temperature at station F.

[redacted]

2408

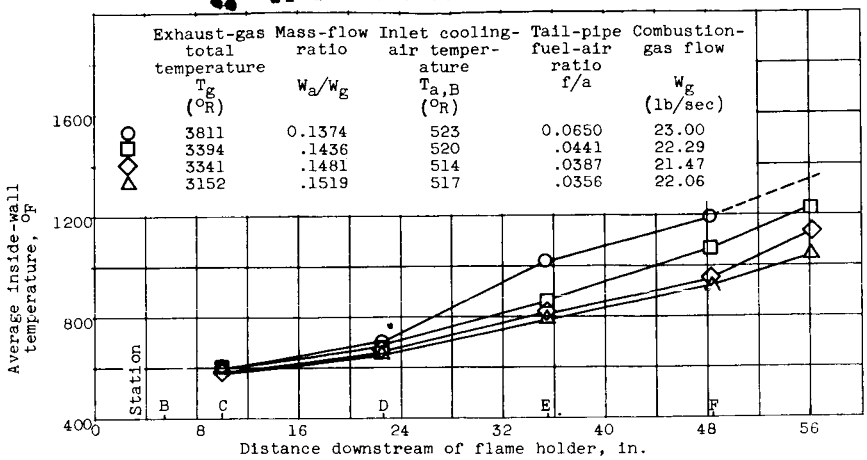

Figure 16. - Effect of exhaust-gas temperature on longitudinal profiles of average inside-wall temperature for configuration A.

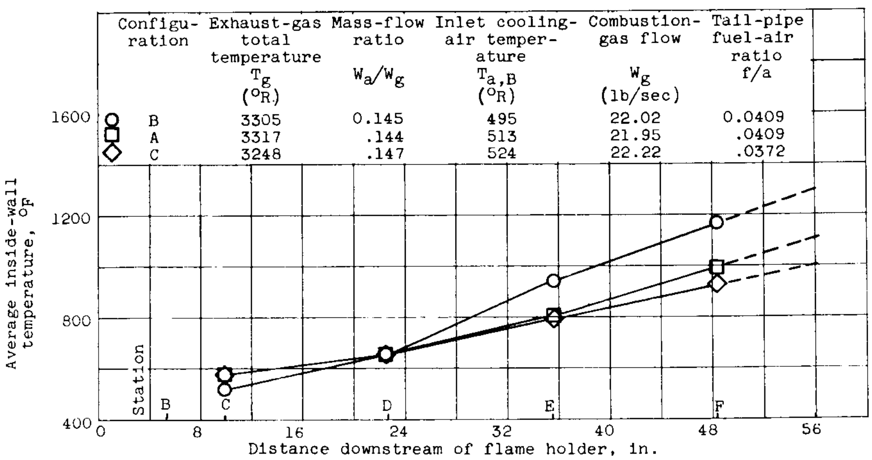

Figure 17. - Effect of fuel distribution on longitudinal profile of average inside-wall temperature.

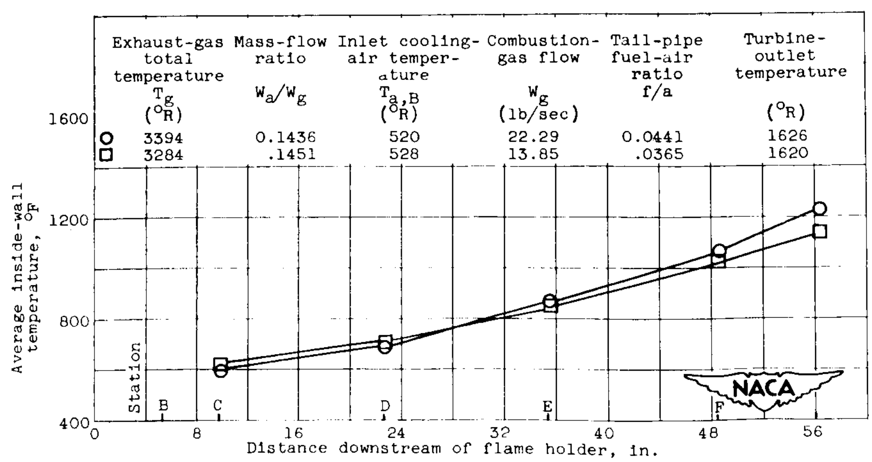

Figure 18. - Effect of combustion-gas mass flow on longitudinal profile of inside-wall temperature for configuration A.

[redacted]

2408

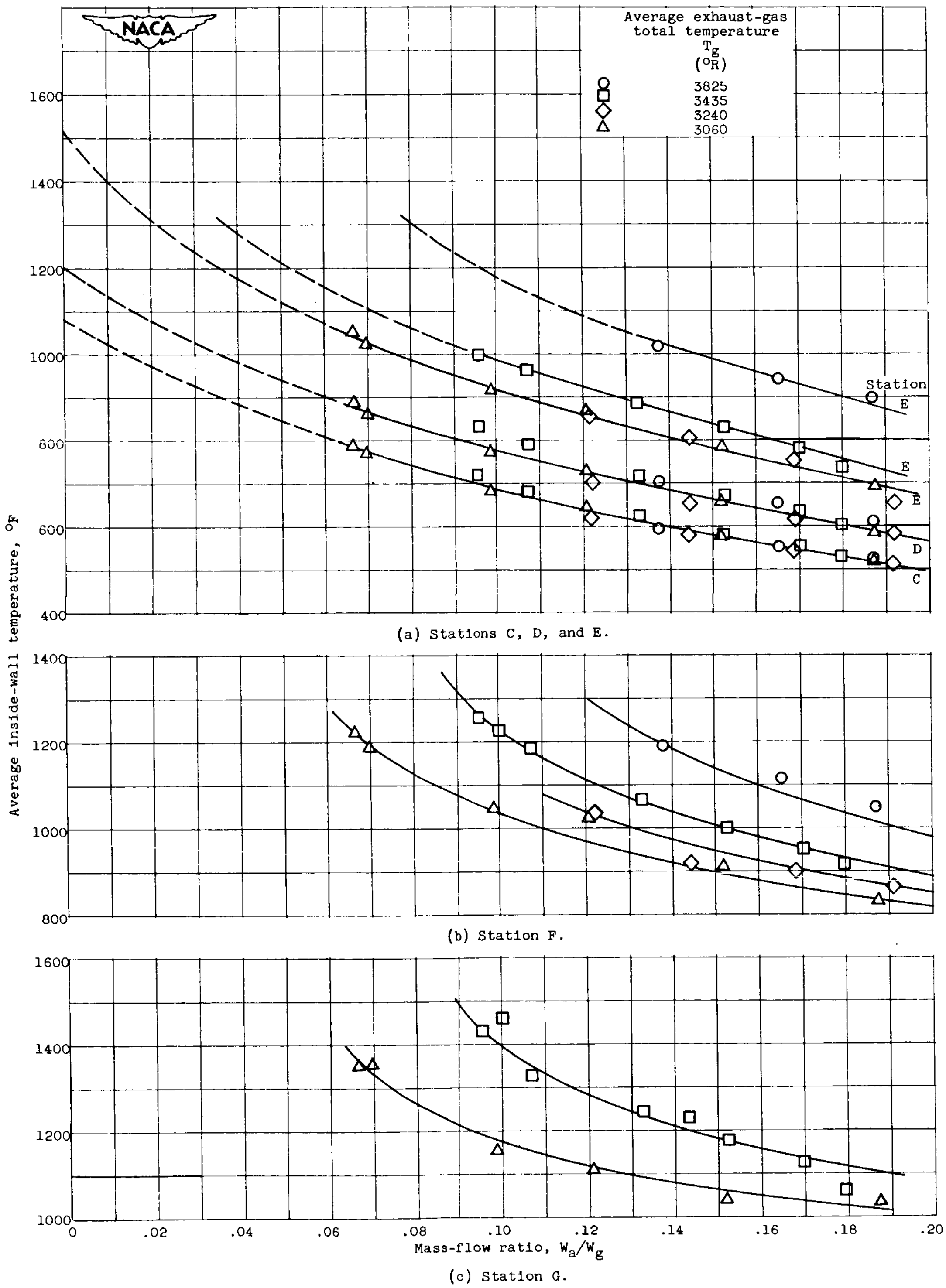

Figure 19. - Variation of average inside-wall temperature with mass-flow ratio of cooling air to combustion gas for configuration A. Approximate inlet cooling-air temperature, 520° R.

[redacted]

2408

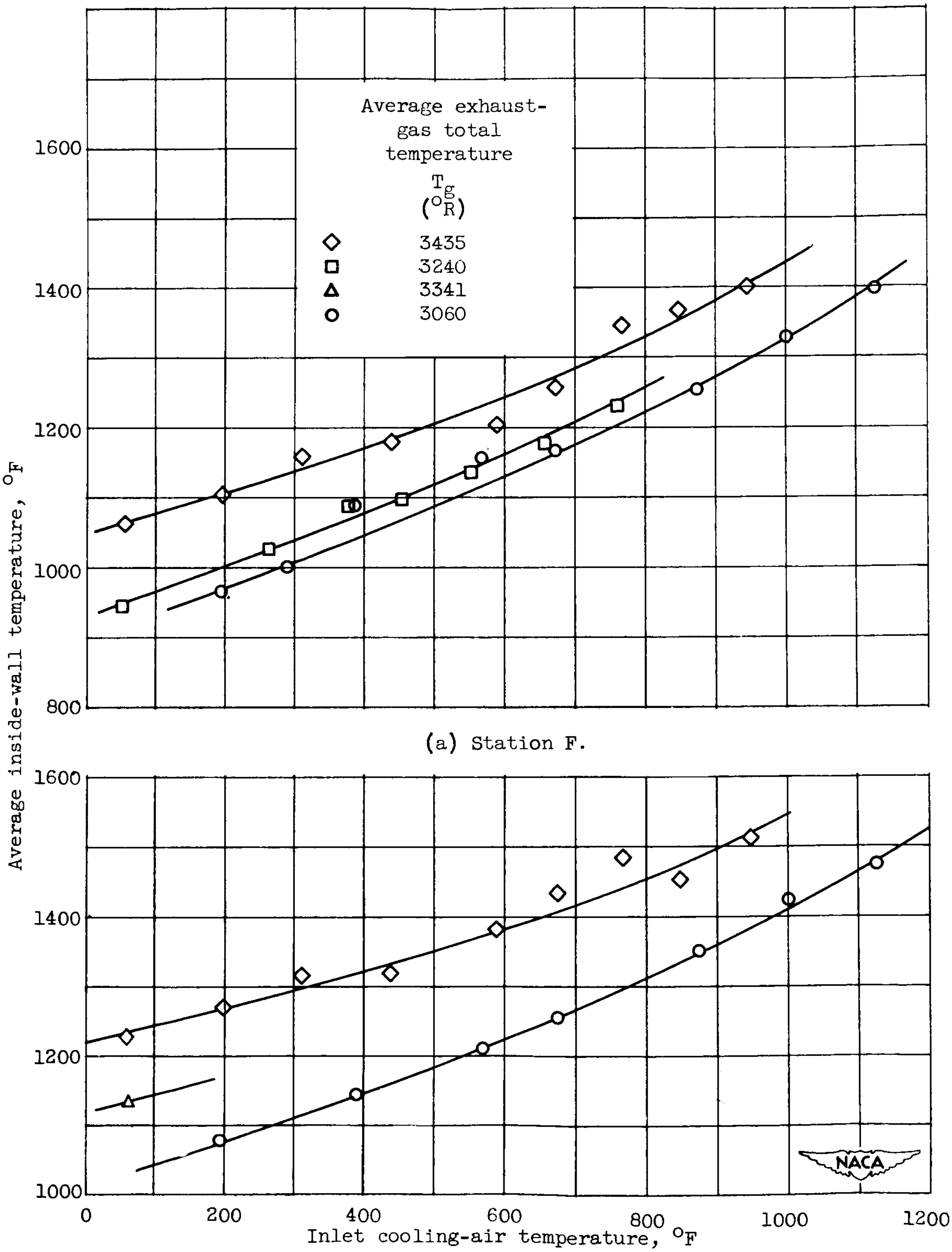

(a) Station F.

(b) Station G.

Figure 20. - Variation of inside-wall temperature with inlet cooling-air temperature for confi[redacted]ss-flow ratio, 0.145.

[redacted]

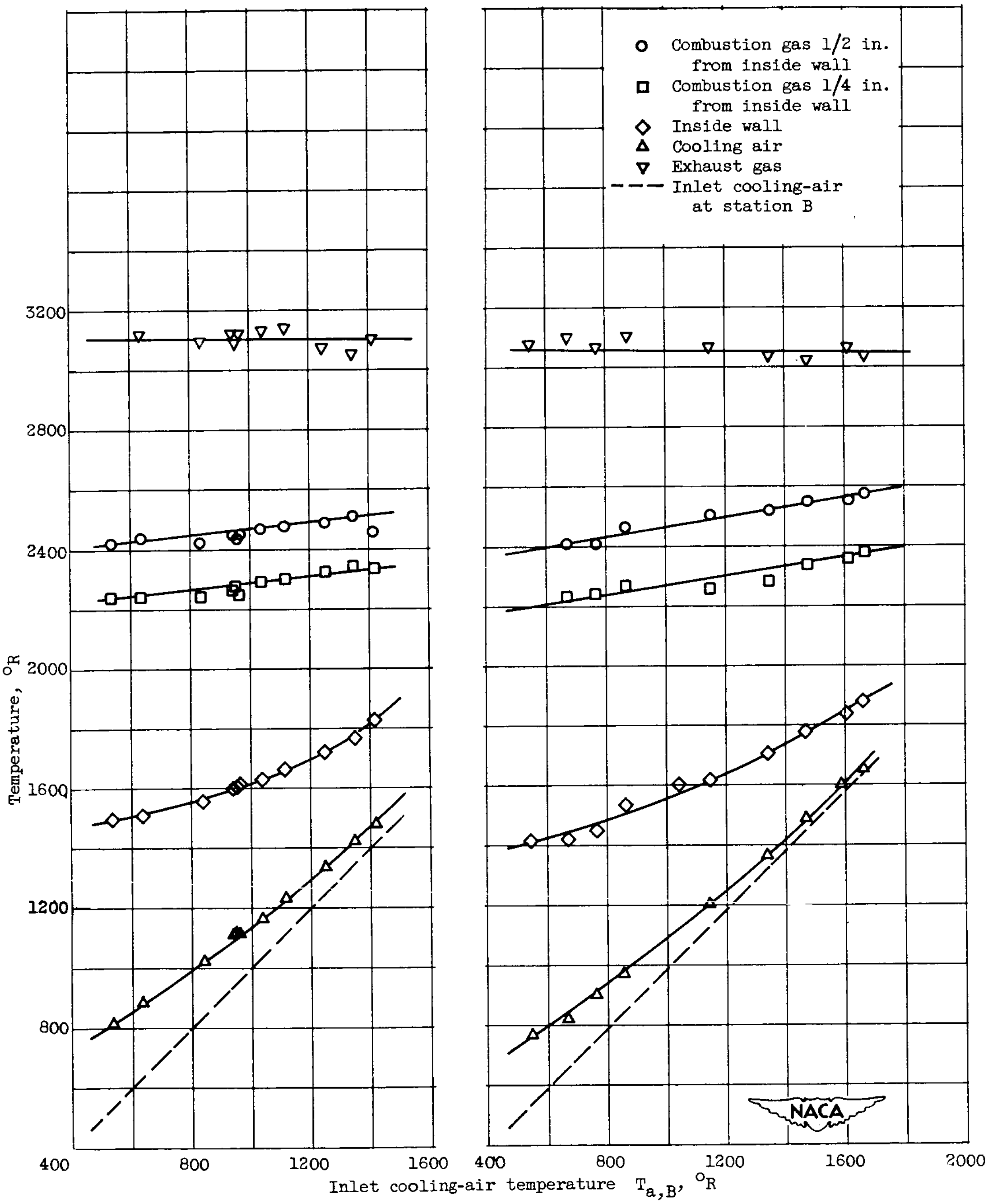

(a) Configuration A; exhaust-gas temperature, 3064° R; combustion-gas flow, 22.3 pounds per second; mass-flow ratio, 0.098.

(b) Configuration A; exhaust-gas temperature, 3095° R; combustion-gas flow, 22.3 pounds per second; mass-flow ratio, 0.148.

Figure 21. - Relation of temperatures at station F.

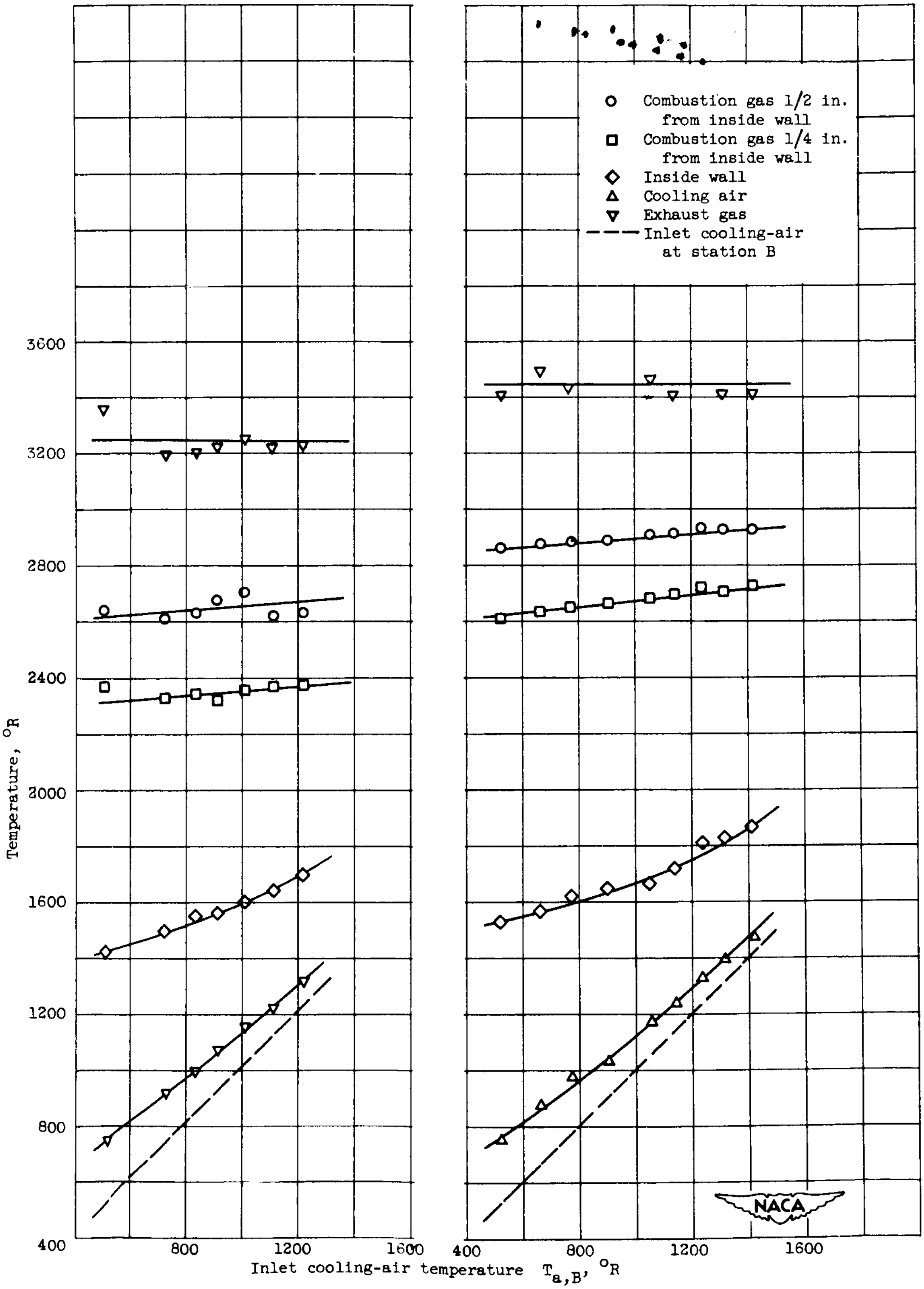

(c) Configuration A; exhaust-gas temperature, 3224° R; combustion-gas flow, 22.3 pounds per second; mass-flow ratio, 0.143.

(d) Configuration A; exhaust-gas temperature, 3422° R; combustion-gas flow, 22.3 pounds per second; mass-flow ratio, 0.143.

Figure 21. - Continued. Relation of temperatures at station F.

[redacted]

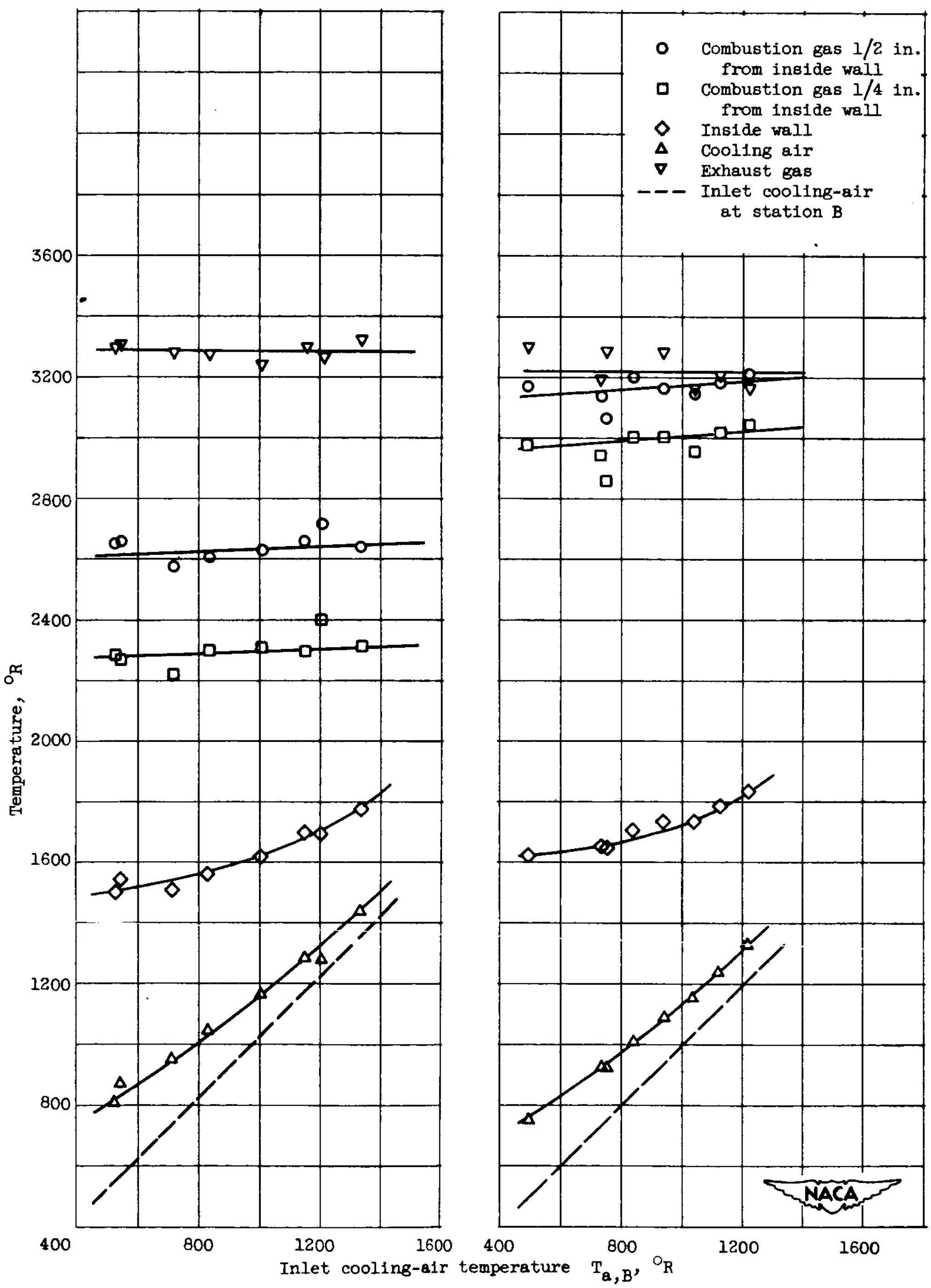

(e) Configuration A; exhaust-gas temperature, 3265° R; combustion-gas flow, 13.8 pounds per second; mass-flow ratio, 0.143.

(f) Configuration B; exhaust-gas temperature, 3225° R; combustion-gas flow, 22.3 pounds per second; mass-flow ratio, 0.144.

Figure 21. - Continued. Relation of temperatures at station F.

[redacted]

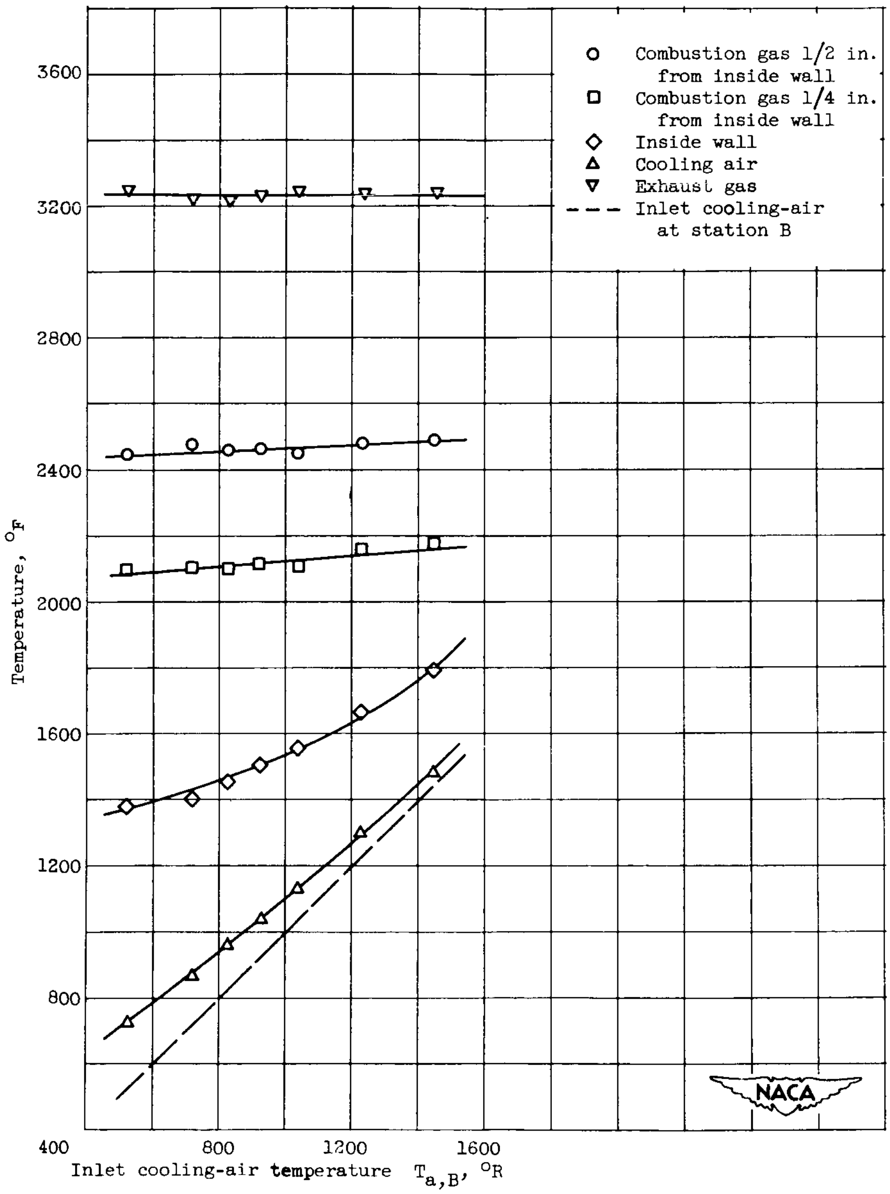

(g) Configuration C; exhaust-gas temperature, 3235° R; combustion-gas flow, 22.3 pounds per second; mass-flow ratio, 0.143.

Figure 21. - Concluded. Relation of temperatures at station F.

[redacted]

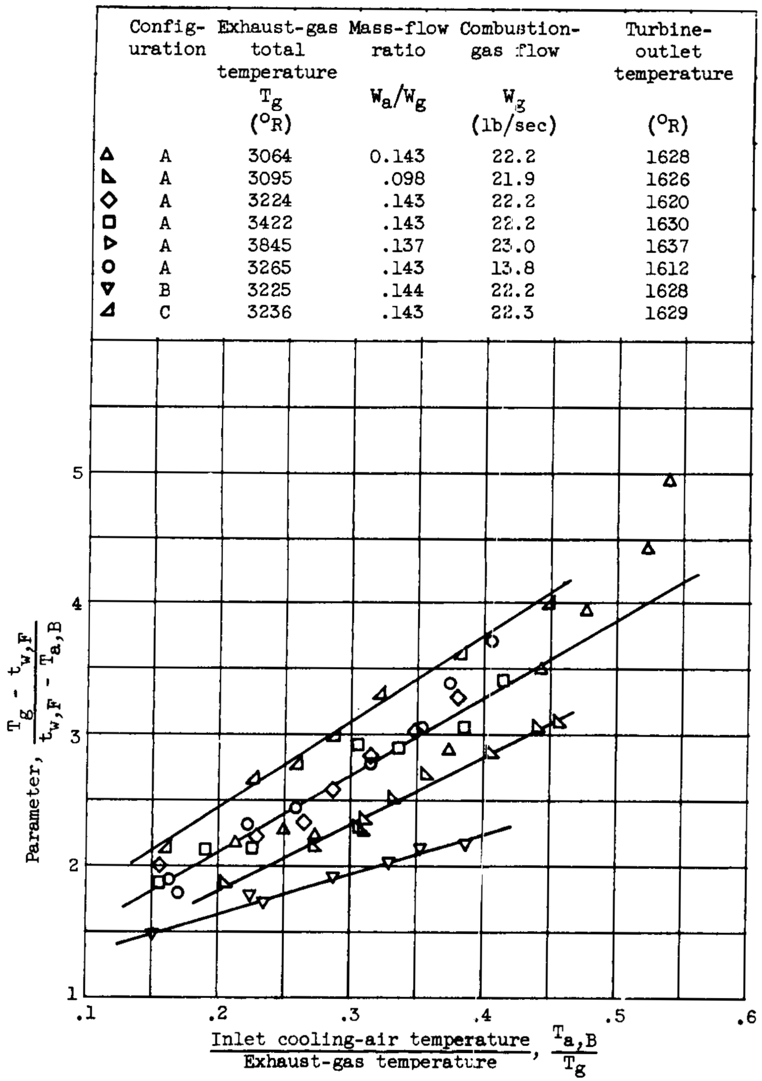

Figure 22. - Comparison of effects of exhaust-gas temperature level, radial distribution of tail-pipe fuel flow, and mass-flow ratio on cooling characteristics.

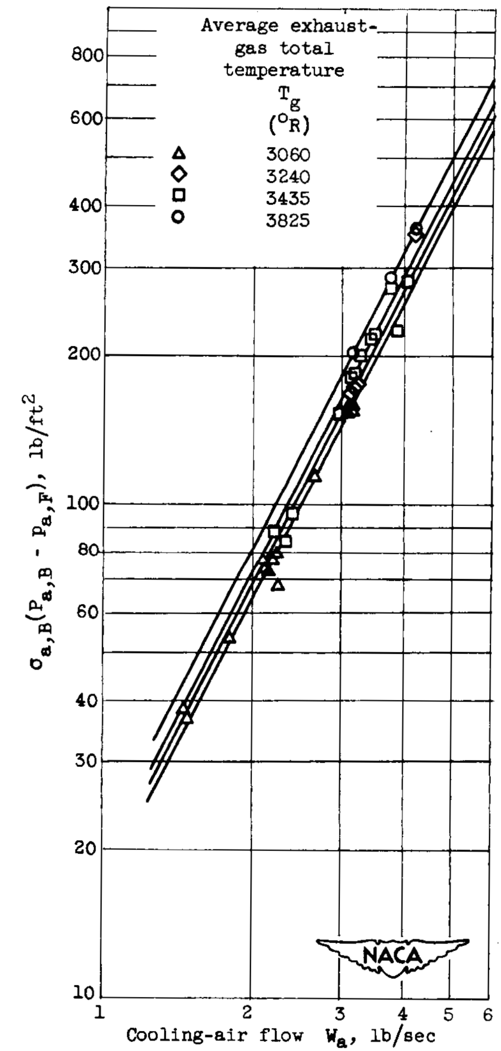

Figure 23. - Correlation of cooling-air pressure drop.

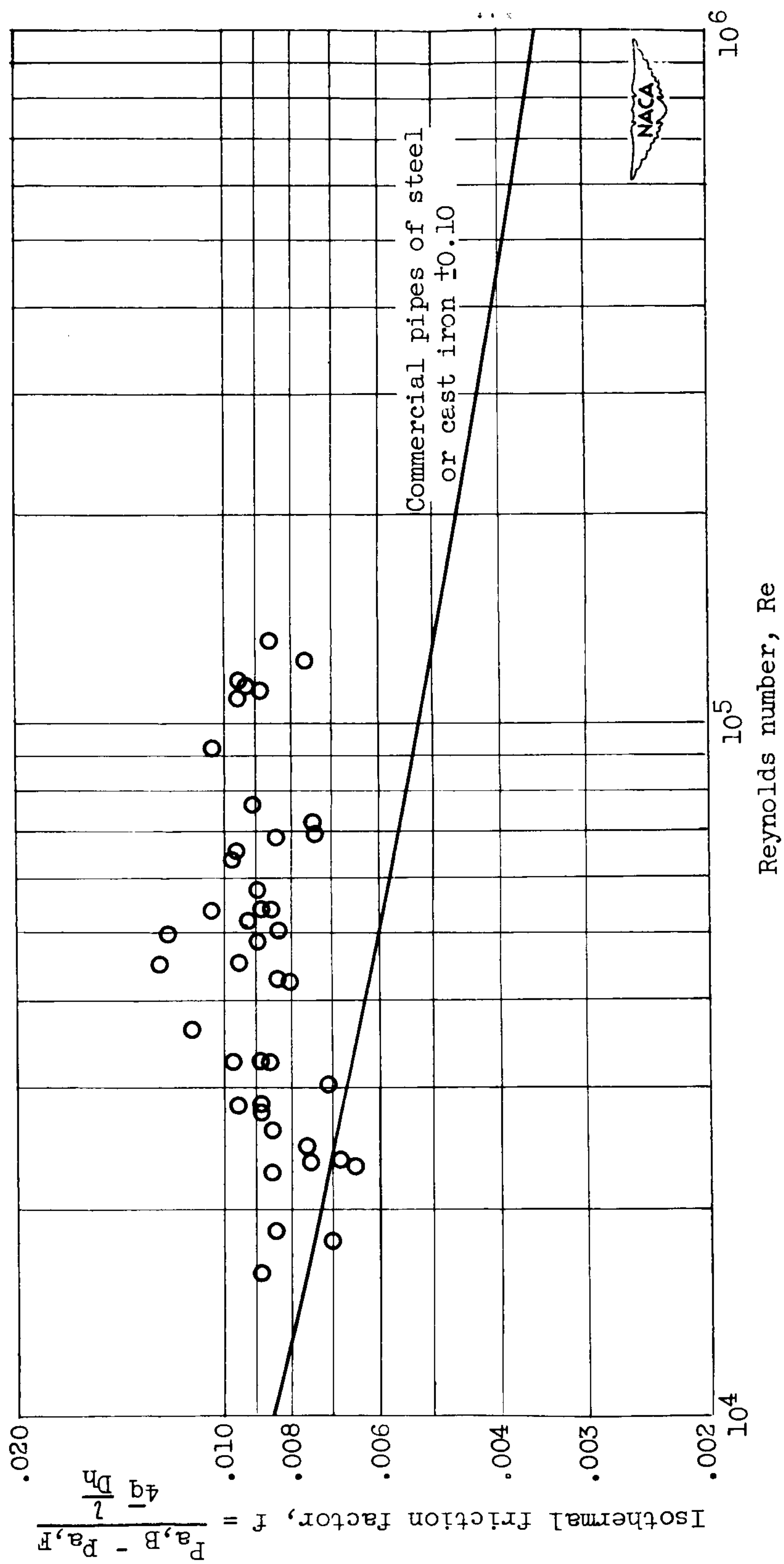

Figure 24. - Isothermal friction factor for instrumented cooling passages.

[redacted]